PENNSTATE

DEPARTMENT OF METEOROLOGY

AFOSR-TR- 88-0778

Long Term Studies of the Refractive Index Structure Parameter in the Troposphere and Stratosphere

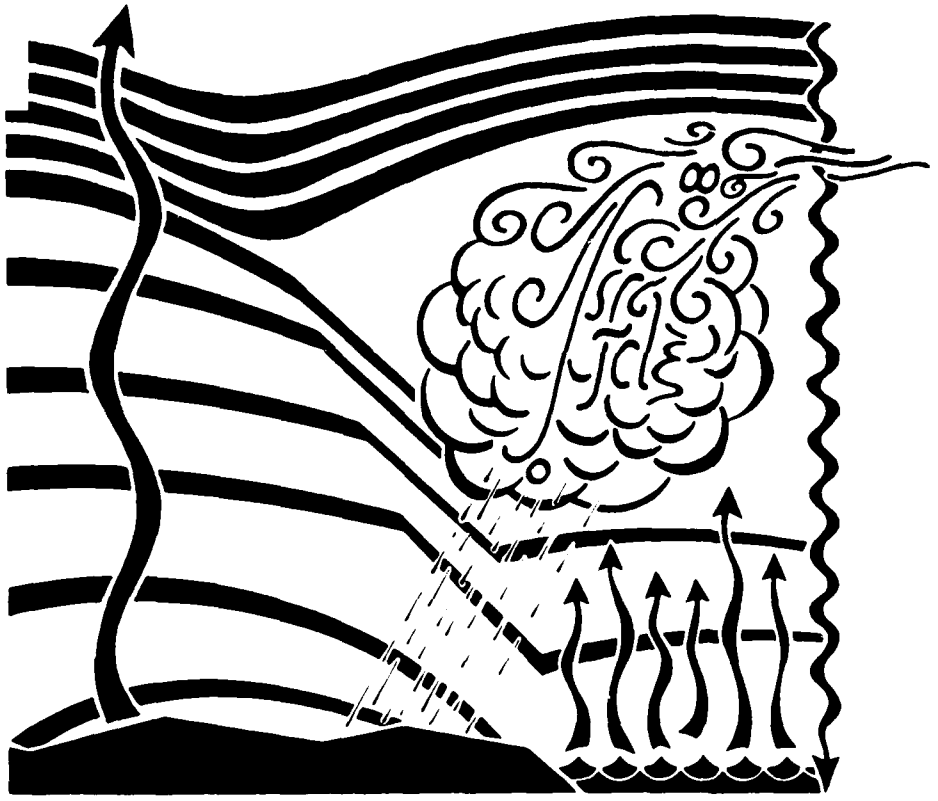

C.W. Fairall
D.W. Thomson
and
W.J. Syrett

Department of Meteorology

The Pennsylvania State University
University Park, PA 16802

Final Report
Air Force Office of Scientific Research
Directorate of Chemical and Atmospheric Sciences
Bolling AFB, DC 20332-6448

Contract AFOSR-86-0049

UNCLASSIFIED
SECURITY CLASSIFICATION OF THIS PAGE

ADA198313

REPORT DOCUMENTATION PAGE

Form Approved
OMB No. 0704-0188

1a. REPORT SECURITY CLASSIFICATION Unclassified	1b. RESTRICTIVE MARKINGS
2a. SECURITY CLASSIFICATION AUTHORITY	3. DISTRIBUTION/AVAILABILITY OF REPORT Approved for public release; Distribution unlimited
2b. DECLASSIFICATION/DOWNGRADING SCHEDULE	
4. PERFORMING ORGANIZATION REPORT NUMBER(S)	5. MONITORING ORGANIZATION REPORT NUMBER(S) AFOSR-TR- 88-0778
6a. NAME OF PERFORMING ORGANIZATION Pennsylvania State University 6b. OFFICE SYMBOL (If applicable)	7a. NAME OF MONITORING ORGANIZATION AFOSR/NC
6c. ADDRESS (City, State, and ZIP Code) Dept. of Meteorology 503 Wlaker Bldg. University Park, PA 16802	7b. ADDRESS (City, State, and ZIP Code) Building 410 Bolling AFB, DC 20332-6448
8a. NAME OF FUNDING/SPONSORING ORGANIZATION AFOSR 8b. OFFICE SYMBOL (If applicable) NC	9. PROCUREMENT INSTRUMENT IDENTIFICATION NUMBER AFOSR-86-0049
8c. ADDRESS (City, State, and ZIP Code) Building 410 Bolling AFB, DC 20332-6448	10. SOURCE OF FUNDING NUMBERS PROGRAM ELEMENT NO. 61102F; PROJECT NO. 2310; TASK NO. A1; WORK UNIT ACCESSION NO.

11. TITLE (Include Security Classification)
Long Term Studies of the Refractive Index Structure Parameter in the Troposphere and Stratosphere

12. PERSONAL AUTHOR(S)
C. W. Fairall, D. W. Thompson, and W. J. Syratt

13a. TYPE OF REPORT	13b. TIME COVERED	14. DATE OF REPORT (Year, Month, Day)	15. PAGE COUNT
FINAL	FROM 11/85 TO 4/88		72

16. SUPPLEMENTARY NOTATION

17. COSATI CODES			18. SUBJECT TERMS (Continue on reverse if necessary and identify by block number)
FIELD	GROUP	SUB-GROUP	

19. ABSTRACT (Continue on reverse if necessary and identify by block number)

SEE REVERSE

20. DISTRIBUTION/AVAILABILITY OF ABSTRACT	21. ABSTRACT SECURITY CLASSIFICATION
☒ UNCLASSIFIED/UNLIMITED ☐ SAME AS RPT. ☐ DTIC USERS	Unclassified

22a. NAME OF RESPONSIBLE INDIVIDUAL	22b. TELEPHONE (Include Area Code)	22c. OFFICE SYMBOL
Lt Col James P. Koermer	(202) 767-4960	NC

DD Form 1473, JUN 86 — Previous editions are obsolete. — SECURITY CLASSIFICATION OF THIS PAGE

UNCLASSIFIED

88 8 25 155

This project was concerned with the relation of meteorological conditions to parameters and processes that influence the optical propagation properties and establishment of a climatology of refractive index structure function parameter as measured with a network of doppler radars. The relation of the atmospheric turbulence profile to the synoptic context and physical models to predict the profile using standard meteorological profile data was also being investigated. The study features two modes of data archiving: (1) continuous archiving of 1 hr average wind profiles and turbulence levels, and (2) high time resolution measurements in association with other measurements (ground-based optical scintillometers, aircraft or radiosondes) in an intensive 'campaign' given the acronym EWAK.

The atmospheric turbulence profiles and resultant optical propagation parameters have been found to be strongly influenced by synoptic conditions. In particular, the turbulence was substantially affected by to strength and location of the jetstream. A very strong correlation between wind shear (which was maximum above and below the core of the jet) and pilot reports of turbulence was found. Richardson number gave a much weaker indication, possibly because of the poorer quality of the vertical temperature gradient data. A comparison of five different methods (four measurement and one model) of obtaining optical C_n^2 showed average disagreements as large as a factor of three. A study of the ratio of temperature to velocity microturbulence showed that the assumption of a constant mixing efficiency (used in the Van Zandt model) may not be valid for very weak turbulence. The potential for using operational numerical forecast models to compute turbulence estimates from predicted wind and temperature profiles was examined in a preliminary look at the ability of the NMC neated Grid Model (NGM) to reproduce the wind speed and direction directly measured by the radars. The standard deviation between the radar and model was on the order of 6 m/s for wind speed and 15 degrees for wind direction at the initial analysis time. The uncertainty in wind direction increased to about 25 to 30 degrees for a 48 hr forecast but the uncertainty in wind speed did not change significantly. A systematic difference of several m/s was found during the winter, probably due to over smoothing of mesoscale features by the model.

AFOSR-TR- 88-0778

COMPLETED PROJECT SUMMARY

1. TITLE: Long Term Studies of the Refractive Index Structure Parameter In the Troposphere and Stratosphere

2. PRINCIPAL INVESTIGATORS: C.W. Fairall and D.W. Thomson
Department of Meteorology
505 Walker Building
The Pennsylvania State University
University Park, PA 16802

3. INCLUSIVE DATES: 15 November 1985 - 15 March 1988

4. GRANT NUMBER: AFOSR-86-0049

5. COSTS AND FY SOURCE: $146,419, FY 86; $111,358, FY 87

6. SENIOR RESEARCH PERSONNEL: None

7. JUNIOR RESEARCH PERSONNEL: Robert Peters, Scott Williams, William Syrett

8. PUBLICATIONS:

Williams, S.R. and D.W. Thomson, 1986: An evaluation of errors observed in the measurement of low wind velocities. Handbook for MAP, Vol. 20 , SCOSTEP secretariat, Dep. Elec. Comp. Eng., Univ. IL., 256-262.

Williams, S.R., and R. Peters, 1986: The Penn State doppler network progress report. Handbook for MAP, Vol. 20 , SCOSTEP secretariat, Dep. Elec. Comp. Eng., Univ., IL., 339-341.

Moss, M.T., 1986: Measurement and modeling of tropospheric/stratospheric refractive index structure parameter. PhD thesis prospectus, Florida State University.

Beecher, E.A., 1987: Analysis of temperature and velocity microturbulence parameters from aircraft data and relation to atmospheric refraction index structure. M.S. Thesis, Pennsylvania State University, pp165.

Syrett, W.J., 1987: Some applications of 50 MHz wind profiler data: detailed observations of the jet stream. M.S. thesis, Pennsylvania State University, pp135.

Fairall, C.W., 1987: A top-down and bottom-up diffusion model of C_T^2 and C_q^2 in the entraining convective boundary layer. J. Atmos. Sci., 44, 1009-1017.

Thomson, D.W., W.J. Syrett, T.T. Warner, and N.L. Seaman, 1988: Proc. 8th Conf. on Numerical Weather Prediction, AMS, Feb. 22-25, Baltimore, MD, pp6.

Fairall, C.W., D.W. Thomson and R. Markson, 1988: An aircraft and radar study of temperature and velocity microturbulence in the stably stratified free troposphere. Proc. 8th Symposium on Turbulence and Diffusion, AMS, April 24-29,San Diego, CA,61-65.

Williams, S.A. and D.W. Thomson, 1988: Comparisons between Wind Profiler and conventional Loran/Omega based rawinsonde wind measurements. In preparation.

9. ABSTRACT OF OBJECTIVES AND ACCOMPLISHMENTS

This project is concerned with the relation of meteorological conditions to parameters and processes that influence the optical propagation properties of the turbulent atmosphere. The approach is centered around the establishment of a climatology of refractive index structure function parameter as measured with a network of doppler radars. The relation of the atmospheric turbulence profile to the synoptic context and physical models to predict the profile using standard meteorological profile data is also being investigated. The study features two modes of data archiving: (1) continuous archiving of 1 hr average wind profiles and turbulence levels, and (2) high time resolution measurements in association with other measurements (ground-based optical scintillometers, aircraft or radiosondes) in an intensive 'campaign' given the acronym EWAK.

The atmospheric turbulence profiles and resultant optical propagation parameters have been found to be strongly influenced by synoptic conditions. In particular, the turbulence is substantially affected by to strength and location of the jetstream. A very strong correlation between wind shear (which is maximum above and below the core of the jet) and pilot reports of turbulence was found. Richardson number gave a much weaker indication, possibly because of the poorer quality of the vertical temperature gradient data. A comparison of five different methods (four measurement and one model) of obtaining optical C_n^2 showed average disagreements as large as a factor of three. A study of the ratio of temperature to velocity microturbulence showed that the assumption of a constant mixing efficiency (used in the Van Zandt model) may not be valid for very weak turbulence. The potential for using operational numerical forecast models to compute turbulence estimates from predicted wind and temperature profiles was examined in a preliminary look at the ability of the NMC Nested Grid Model (NGM) to reproduce the wind speed and direction directly measured by the radars. The standard deviation between the radar and model was on the order of 6 m/s for wind speed and 15 degrees for wind direction at the initial analysis time. The uncertainty in wind direction increased to about 25 to 30 degrees for a 48 hr forecast but the uncertainty in wind speed did not change significantly. A systematic difference of several m/s was found during the winter, probably due to over smoothing of mesoscale features by the model.

Final Report

Contract AFOSR-86-0049

Long Term Studies of the Refractive Index Structure Parameter in the Troposphere and Stratosphere

C.W. Fairall, D.W. Thomson, and W.J. Syrett

Department of Meteorology

505 Walker Building

The Pennsylvania State University

University Park, PA 16802

ABSTRACT

This project is concerned with the relation of meteorological conditions to parameters and processes that influence the optical propagation properties of the turbulent atmosphere. The approach is centered around the establishment of a climatology of refractive index structure function parameter as measured with a network of Doppler radars. The relation of the atmospheric turbulence profile to the synoptic context and the use of physical models to predict the profile using standard meteorological profile data is also being investigated. The study features two modes of data archiving: (1) continuous archiving of 1 hr average wind profiles and turbulence levels, and (2) high time resolution measurements in association with other measurements (ground-based optical scintillometers, aircraft or radiosondes) in an intensive 'campaign' given the acronym EWAK.

The atmospheric turbulence profiles and resultant optical propagation parameters have been found to be strongly influenced by synoptic conditions. In particular, the turbulence is substantially affected by to strength and location of the jet stream. A very strong correlation between wind shear (which is maximum above and below the core of the jet) and pilot reports of turbulence was found. Richardson number gave a much weaker indication, possibly because of the poorer quality of the vertical temperature gradient data. A comparison of five different methods (four measurement and one model) of obtaining optical C_n^2 showed average disagreements as large as a factor of three. A study of the ratio of temperature to velocity microturbulence showed that the assumption of a constant mixing efficiency (used in the Van Zandt model) may not be valid for very weak turbulence. The potential for using operational numerical forecast models to compute turbulence estimates from predicted wind and temperature profiles was examined in a preliminary

look at the ability of the NMC Nested Grid Model (NGM) to reproduce the wind speed and direction directly measured by the radars. The standard deviation between the radar and model was on the order of 6 m/s for wind speed and 15 degrees for wind direction at the initial analysis time. The uncertainty in wind direction increased to about 25 to 30 degrees for a 48 hr forecast but the uncertainty in wind speed did not change significantly. A systematic difference of several m/s was found during the winter, probably due to over smoothing of mesoscale features by the model.

ACKNOWLEDGEMENTS

This work was directly supported by the Air Force Office of Scientific Research contract number AFOSR-86-0049; the radar systems were originally obtained on AFOSR-83-0275. Robert Peters and Scott Williams of the Department of Meteorology, PSU, were primarily responsible for the construction and operation of the radars (with external assistance as described in the appendix).

The authors wish to acknowledge Lt. Beth Beecher and Capt. Mike Moss for their contributions to and analysis of the EWAK experiment. Special thanks to Ralph Markson and Bruce Anderson of Airborne Research Associates for their aircraft participation in EWAK and to Don Stebbins of Rome Air for his interest in putting EWAK

CONTENTS

I. Introduction

The importance of turbulence in the atmospheric boundary layer, which is the basic living environment of humankind, has long been recognized. Only in the last few decades has the importance of free atmospheric (i.e., above the boundary layer) turbulence been recognized. Even in the absence of clouds, stably stratified fluids (e.g., the free troposphere and stratosphere) are observed to experience intermittent transitions to turbulent regimes. Although it is referred to as Clear Air Turbulence (CAT) it does occur in regions of stable clouds such alto or cirrostratus. The beautiful breaking wave clouds provide visual evidence of CAT. CAT is important in aircraft performance and safety, optical propagation, EM propagation and communications, atmospheric dispersion of pollutants, and as a source of viscous drag in the 'free' atmosphere.

The atmospheric refractive index structure function parameter, C_n^2, is important in a broad range of optical propagation applications (see Section II). Examples of the consequence of atmospheric microturbulence on optical systems include: reduced intensity (Yura, 1971), beam wander (Fried, 1966), scintillation and coherence (Fried and Schmeltzer,1967), and anisoplanatism (Fried, 1981). The consequences of spatially and temporally varying C_n^2 can be computed for a specific optical system, at least in principle, by specifying the values of C_n^2 along the optical path. While an extensive base of data and theory is available for planetary boundary layer (PBL) properties of C_n^2 (see Fairall et al., 1982; Fairall, 1987), only a few case studies are available for the free troposphere and the lower stratosphere (Walters and Kunkel, 1981). The ALLCAT (i.e., HICAT, MEDCAT, etc.) program of the late 1960's focused primarily on large scale turbulence severe enough to damage aircraft or discomfit passengers. Now the structure and dynamical

properties of both CAT and C_n^2 in the free troposphere and lower stratosphere are receiving renewed attention. For C_n^2 this is because of the recognition of the importance of the isoplanatic angle in the performance of a variety of ground-to-space systems that utilize adaptive optics. Concurrently development of VHF clear air Doppler radars, the performance of which are directly proportional to C_n^2, has rekindled the interest of the meteorological community in the climatology and dynamics of CAT. It turns out that this is still poorly understood. For example, a recent long term study of C_n^2 using VHF radar (Nastrom et al., 1981) revealed substantial diurnal and seasonal variations even in the stratosphere. This study suggested that strong tropospheric convection and the jet stream were relevant factors in the intensity of CAT but, at present, this is only conjecture based on physical plausibility.

The investigation of atmospheric turbulence involves the collection of data, the development of theory and the implementation of models. The data tells us what is 'up there' at the time of the measurement, but the theory and models are true indices of our understanding of the phenomena. With models we attempt to predict an important but difficult to measure variable (e.g., C_n^2) from variables that we expect to have at our disposal (e.g., regional scale radiosonde information). Dynamical models of turbulence based on the Navier-Stokes and turbulent kinetic energy (TKE) equations have a rich tradition in PBL research. Both second order closure and large eddy simulations have provided great insights into the structure of PBL turbulence. In contrast, the only model of CAT in use today is purely statistical in nature (Van Zandt et al., 1981; Moss, 1986).

Remote sensors are ideal for the study of climatological properties of turbulence in the free troposphere and stratosphere. In this regard, the VHF

and UHF Doppler radars are particularly well suited because of their all weather and day/night capabilities. The Penn State Department of Meteorology is now completing a mesoscale triangular network of three VHF radars under funding provided by the DoD (AFOSR) University Research Instrumentation Program. DoD (AFOSR and ONR) funding has also been obtained for the construction of a multichannel mm-wave radiometer system for continuous groundbased measurements of temperature profiles and integrated water vapor/liquid. Subsystems of this radiometer are now being tested. It is expected to be online at Penn State in mid 1988. Finally, a fourth Doppler radar has been constructed. It is a UHF system similar in concept to the VHF systems but operating at 0.75 m rather than 6 m wavelength. The UHF system has a smaller, more portable antenna, better vertical resolution (100 m vs. 300 m for the VHF systems) and far superior low altitude capabilities (minimum range of 200 m). The radar systems are capable of producing a wind and turbulence profile with roughly 30 to 90 second time resolution. Thus, they are also ideal for highly detailed studies of turbulence and its relationship to mesoscale phenomena. The combination of the mesoscale triangle of VHF profilers, the UHF profiler and the radiometers constitutes an atmospheric observing system that represents a quantum jump in our ability to study the atmosphere.

This report describes a two year project to use these systems to study the seasonal and diurnal climatology of C_n^2, the atmospheric dynamical processes responsible for the variability of C_n^2, and to investigate measurement methods and models of C_n^2. The results have been published in the open literature (see section VIII) and in a number of graduate assistant M.S. theses [Beecher (1987), Carlson (1987), Knowlton (1987), Neiman (1987), and Syrett (1987)]. The work combined the full power of the department's

observing systems, access to national data networks and weather/satellite information, and cooperation with a number of government research laboratories. During the study an intensive field program was held at Penn State involving in situ measurements with aircraft and thermosonde balloons and a variety of ground based electro-optical systems (e.g., scintillometers). This study was given the acronym EWAK and involved scientists from a number of DoD laboratories (see section IV). The purpose of EWAK was to compare measurement methods and to test/develop models of clear air turbulence. The emphasis on relating turbulence to mesoscale and synoptic scale structures was intended to promote the extension of the results to different climatological regions. A thorough understanding of these relationships should lead to assessment and forecasting of atmospheric turbulence with a combination of satellite informational and numerical global weather models.

II. Refractive Index of Air

For many purposes the effects of atmospheric gas on propagating electromagnetic and acoustic radiation may be conveniently subdivided into the following subcategories:

a) mean density gradients result in beam refraction and, consequently, tracking or pointing errors,

b) density and velocity fluctuation caused by turbulence produce refractive index variations which, in turn, degrade system performance.

Regarding the bulk radar refractive index, n, of atmospheric gas it is convenient to specify it in terms of the refractivity, $N = (n-1)*10^6$, in which case

$$N = 77.6\ (P + 4810\ e/T)/T \qquad (1)$$

where N, T, P and e are in units of ppm, K, mb (total pressure), and mb (vapor pressure), respectively. The second term including e specifies the contribution by polar molecules (principally water). It is often negligible at optical frequencies where the humidity coefficient is much smaller.

For specification of the effects of turbulence the relevant atmospheric properties are the refractive index structure function parameter, C_n^2, (Tatarski, 1961) and the inner scale or Kolmogorov scale of turbulence, L_k (Livingston, 1972; Hill and Clifford, 1978). C_n^2 can be related to micrometeorological variables by (Wesely, 1976)

$$C_n^2 = A(C_T^2 + 2\ B\ C_{Tq} + B^2 C_q^2) \qquad (2)$$

where A and B are functions of temperature (T), pressure and specific humidity

(q); C_T^2, C_{Tq}, and C_q^2 are the temperature and humidity structure function parameters. The values of A and B are also radiation-type and wavelength dependent. L_k is related to the viscosity and density of air (both functions of altitude) and the rate of dissipation of turbulent kinetic energy, ϵ (Hinze, 1975).

III. Background on Clear Air Turbulence

A. Microturbulence

In general, atmospheric turbulence is anisotropic. However, it is known that at small size scales (large values of wavenumber, k), the eddies become increasingly isotropic. In the isotropic limit it can be shown that (Hinze, 1975) the structure function parameter, C_x^2, for the unspecified variable, X, (X could be u, T, q, or n)

$$C_x^2 = \langle (X(r)-X(r+d))^2 \rangle / d^{2/3} \tag{3}$$

is independent of the spacing, d. In this equation X(r) denotes the value of X at position r while X(r+d) denotes the value at a position a distance d from r; the brackets denote an average. Using dimensional arguments, Kolmogorov showed that in the isotropic limit the one-dimensional variance spectrum obeys a $k^{-5/3}$ wavenumber dependence

$$\varphi_x(k) = \beta_x \chi_x \epsilon^{-1/3} k^{-5/3} \tag{4}$$

where χ_x is the rate of dissipation of <u>one half</u> of the variance of X and β_x is an empirical constant (on the order of 0.5 for velocity and 0.8 for scalars). It can similarly be shown that

$$\varphi_x(k) = 0.25\, C_x^2\, k^{-5/3} \tag{5}$$

where the factor 0.25 represents several mathematical constants. Note that (4) and (5) imply the Corrsin relation

$$C_x^2 = 4\ \beta_x \chi_x \epsilon^{-1/3} \tag{6}$$

Velocity is a special case (since $\chi_u = \epsilon$) so that

$$C_u^2 = 2.0\ \epsilon^{2/3} \tag{7}$$

B. TKE and Variance Budget Equations

The simplified, horizontally homogeneous budget equations for TKE (symbol E) and scalar variance (symbol $\langle x^2 \rangle$), are

$$DE/Dt = -\langle uw \rangle \partial U/\partial z + (g/\theta)\partial\theta/\partial z - \epsilon + \text{transport} \tag{8a}$$

$$D(\langle x^2 \rangle/2)/Dt = -\langle xw \rangle \partial X/\partial z - \chi_x + \text{transport} \tag{8b}$$

where the small symbols denote turbulent fluctuations and the capital symbols denote average values, U is the streamwise velocity, W the vertical velocity, g the acceleration of gravity, θ the potential temperature and z the altitude. Assuming a state of dynamic equilibrium, neglecting transport, and using an eddy diffusion coefficient, K, to express the covariance term

$$\langle uw \rangle = -K_m \partial U/\partial z \tag{9a}$$

$$\langle xw \rangle = -K_x \partial X/\partial z \tag{9b}$$

we can use (8) to express the dissipations

$$\epsilon = K_m(\partial U/\partial z)^2 \, [1 - Ri/Pr] \tag{10a}$$

$$\chi_x = K_x(\partial X/\partial z)^2 \tag{10b}$$

where $Pr=K_m/K_H$ is the turbulent Prandtl number and Ri is the gradient Richardson number

$$Ri = N^2/S \tag{11}$$

The factor S is the square of the vertical gradient of the vector mean wind and N is the Brunt-Vaisala frequency, which in the atmosphere is approximately given by

$$N^2 = (g/\theta) \, \partial\theta/\partial z \tag{12}$$

Using (10) we can obtain the ratio of the scalar dissipation to the TKE dissipation

$$\chi_x/\epsilon = (\beta_u/\beta_x) \, C_x^2 \, /C_u^2 = [(\partial X/\partial z)^2/N^2] \, Ri/(Pr-Ri) \tag{13}$$

In the oceanographic literature (Gregg, 1987), this is expressed in terms of the mixing coefficient, γ,

$$\gamma_x = \chi_x N^2/[(\partial X/\partial z)^2 \epsilon] \tag{14}$$

In actively turbulent layers with $Pr \simeq 1$ and $Ri \simeq 0.25$, (13) implies $\gamma = Ri/(Pr-Ri) \simeq 1/3$. Gossard and Frisch (1987) have used the shear budget

equations to show that $\beta_x\gamma/\beta_u \simeq 3/2$ while Gage and Nastrom (1986) have shown that equipartition of two-dimensional TKE and potential energy due to gravity wave displacements in a stratified fluid implies $\beta_x\gamma_\theta/\beta_u = 2$ for large scale (anisotropic) turbulence. As we shall discuss later, relations derived from (13) have been used to compute ϵ and K_m from clear air radar data.

C. Clear Air Turbulence Length Scales

The field of turbulence contains a bewildering variety of length scales which we will not attempt to discuss here. For our purposes, we focus on the smallest scales present, the Kolmogorov microscale L_k, and the scale of the dominant vertical motions (eddy overturning scale) L_o, which is related to the integral scale calculated from the vertical velocity autocorrelation function. At the Kolmogorov scale, viscosity is rapidly destroying the turbulent fluctuations; the spectrum begins to deviate from the -5/3 behavior at sizes an order of magnitude larger than this (Hill and Clifford, 1978). In stratified turbulence, the overturning scale is proportional to the buoyancy length scale, L_b (Gregg, 1987), also referred to as the Ozmidov scale. In terms of the turbulent parameters, these scales are

$$L_k = (\upsilon/\epsilon^3)^{1/4} \tag{15a}$$

$$L_b = (\epsilon/N^3)^{1/2} \tag{15b}$$

The inertial subrange occurs for those size scales smaller than L_b and greater than L_k. If $L_b \simeq L_k$, then the energy containing vertical motions are rapidly destroyed by viscosity; if $L_b \simeq 10L_k$, then no inertial subrange is anticipated.

The ratio of the length scales forms a natural activity parameter to

classify the turbulent state (Gibson, 1987)

$$A = (L_b/L_k)^{4/3} = \epsilon/(\upsilon N^2) \tag{16}$$

Gregg (1987) suggests the following empirical classifications

Value of A	Turbulent State
A<15	Decaying turbulence, $\langle wu\rangle=\langle w\theta\rangle\simeq 0$
A>200	Isotropic
A>10000	Fully developed

The physical interpretation of the mixing coefficient and the activity parameter can be illustrated by noting that the turbulent diffusivity can be expressed as $K_x=A_t\gamma_x\upsilon$. Thus, when the product of the activity parameter and the mixing coefficient exceeds one, then the turbulent mixing processes are more efficient than molecular diffusivity.

The concept of length scales is also used to eliminate the eddy diffusion coefficients from (10) by invoking mixing length theory (Hinze, 1975)

$$K = c_1 E^{1/2} L_o \tag{17}$$

where c_1 is an empirical constant and the square root of E represents a velocity scale. The dissipation is also related to these quantities

$$\epsilon = c_2 E^{3/2}/L_o \tag{18}$$

These relations can be used in (10) to yield

$$C_u^2 = 2\,\epsilon^{2/3} = 2\,(c_1/c_2^{1/3})\,(\partial U/\partial z)^2\,L_o^{4/3} \tag{19a}$$

$$C_x^2 = 2\,(\beta_x/\beta_u)\,(c_1/c_2^{1/3})/(Pr-Ri)\,(\partial X/\partial z)^2\,L_o^{4/3} \tag{19b}$$

Notice that (19a) can be manipulated to give

$$\epsilon/N^3 = (c_1^{3/2}/c_2^{1/2})/Ri^{3/2}\,L_o^2 = L_b^2 \tag{20}$$

The most common convention is to fix the ratio $c_1/c_2^{1/3}=1$ and to assume that in actively turbulent layers $Ri\simeq 0.25$. This implies that $L_o=0.35\,L_b$ (Hocking, 1982). Because the constants are chosen arbitrarily, there is no physical significance to this particular ratio of L_o to L_b. Since L_b is considered to be the outer limit of the validity of the inertial subrange, it makes sense that the true integral scale and the energy containing scale are larger than L_b. It is also clear that application of these expressions is likely to be confused by our inability to be sure of the values of Pr and Ri and by the fact that the assumptions of stationarity and negligible transport will not be valid in all conditions.

D. Statistical Models of C_n^2

Van Zandt et al. (1978,1981) have developed a model of C_n^2 based on a statistical integration of simplified forms of (19). In this approach, a smooth mean profile with a vertical resolution roughly equivalent to a rawinsonde is the input. Velocity and temperature (and, therefore, shear and temperature gradient) fluctuations are allowed (relative to the mean profile) with probability distributions obtained from a mix of empirical analysis and theory about gravity wave effects. Active turbulent regions are assumed to

exist when the fluctuations produce Ri<0.25. By integrating the joint probability distribution over shear, temperature gradient, and size scale space, an average value, $\langle C_n^2 \rangle$, is computed.

The value of $\langle C_n^2 \rangle$ obtained in this manner is the expected value at some altitude; as such, it does not actually contain any information about the vertical distribution. We can see that, at any specific time, quite different results for C_n^2 can be obtained from measurements depending on the vertical resolution. Suppose that the vertical resolution (e.g., a radar range gate of several hundred meters) is much greater than the turbulent patch thickness, H. In this case, we would expect that the radar produces sufficient averaging to be consistent with model assumptions. A high resolution radar, or a high vertical resolution in situ measurement (e.g., an aircraft flying at constant altitude) is likely to produce a measurement that is either in an inactive region or in an active region. Thus a high resolution measurement at a particular altitude may require averaging over a long period of time to be consistent with the model. The time required would be many times longer than the typical lifetime of an actively turbulent layer, which appears to be on the order of a few hours (Syrett, 1987; also, see the discussion in Section III-F).

In an earlier paper Van Zandt et al. (1978) examined this issue with their statistical model by computing the probability of turbulence occurring at a fixed altitude, F. This has been interpreted by some (e.g., Weinstock, 1981) as the expected fraction of a range gate of thickness, 2Δ, that is occupied by turbulence of average scale, $L_b \approx L_o$, i.e., $F \approx L_b/(2\Delta)$. Obviously, this assumes that the patch thickness is much less than the range gate thickness and that only one layer is likely to occur per range gate. Thus, average measurements produced in this fashion are interpreted as

$$\langle \epsilon \rangle = F\ \epsilon \tag{21a}$$

$$\langle C_x^2 \rangle = F\ C_x^2 \tag{21b}$$

where the values on the right hand side represent data within the active layers where Ri≈0.25. While the value of F depends on the mean conditions, Gage et al. (1980) use the model to show that $F^{1/3}N^2$ is approximately constant and has the value of $4*10^{-5}$ in the troposphere and $8*10^{-5}$ in the stratosphere.

The Van Zandt model has never been tested in detail. It has been evaluated by comparing radar measured C_n^2 with predictions from rawinsondes. In a few cases, optical and in situ data have also been used. On average, the model does quite well for C_n^2; this is not shocking because the model originally contained one unspecified constant which was selected to fit radar data. The internal details of the model, such as the probability distributions for shear, N, and F, have not been evaluated. Also, the model appears to overpredict ϵ by two orders of magnitude (Fairall and Markson, 1984). Even the model predictions of C_n^2 have never been examined for a large data set. Furthermore, the model is incomplete in that it provides information about the probability of observing turbulence (F) and, perhaps, the typical size scale of the turbulence ($\langle L_o \rangle$), but it tells us nothing about the vertical distribution of turbulent regions nor does it guarantee that the patch size (H) is the same as L_o. Observations in the ocean (Gregg, private communication) and in the atmosphere (Barat and Bertin, 1984) show that $H \gg L_o$.

E. Inactive Regions

The Van Zandt model partitions the atmosphere vertically into regions with active turbulence (Ri<0.25) and regions that are considered to be nonturbulent (or the turbulence makes a negligible contribution to the average of C_n^2). By inactive, we mean that there is no production of TKE or variance which implies that the covariance terms in (9) must be zero. This condition is met when the activity parameter is less than 15. Thus, we can define a threshhold value (Gibson, 1987) for the dissipation rate, ϵ_t, such that values of ϵ less than ϵ_t imply decaying turbulence,

$$A_t = \epsilon_t/(\upsilon N^2) = 15 \tag{22}$$

A typical value in the free troposphere is $\epsilon_t \simeq 5*10^{-8}$ $m^2 s^{-3}$. Even if A>15 the turbulence may be decaying if the destruction terms exceed the production terms. Sometimes the term 'fossil' turbulence is used to describe this state although that term is also applied to residual temperature structure that remains after the velocity turbulence has been consumed.

Decaying turbulence has been extensively studied in the laboratory using flow through grids (e.g., Itsweire et al., 1986). Atmospheric studies are quite rare, although Nieuwstadt and Brost (1986) performed a large eddy simulation model study of the decay of convective turbulence. We can use the TKE budget equation to analyze decaying turbulence, where we drop the production terms

$$\partial E/\partial t = -\epsilon \tag{23}$$

However, if we eliminate E with (18), then we obtain a differential equation for ϵ

$$d\epsilon/\epsilon^{4/3} = -(3/2)\ (c_2/L_o)^{2/3}\ dt \tag{24}$$

If we assume that the size scale remains constant throughout the decay process then (24) has the solution

$$\epsilon = \epsilon_o\ (1 + t/t_o)^{-3} \tag{25}$$

where ϵ_o is the value of ϵ at the beginning of the decay process and t_o is

$$t_o = 2\ [L_o^2/(c_2^2\ \epsilon_o)]^{1/3} \simeq c_2^{-2/3}\ N^{-1} \tag{26}$$

Measurements in the ocean (Dillon, 1982) suggest $t_o N \simeq 0.3$, which implies that an inactive region has a turbulent lifetime that is only on the order of a Brunt-Vaisala period. However, this is the value of Brunt-Vaisala period within the turbulent layer itself, which may be much longer (because of mixing) than the value associated with the mean background temperature profile (about two minutes in the atmosphere).

F. Active Regions

The dynamics and time scales of regions of active turbulence are fairly complicated and very little complete data is available to aid in the analysis. It is generally conceded that the turbulence is initiated by Kelvin-Helmholtz instability when the Richardson number decreases to a value near 0.25. Several physical processes are able to cause this decrease. Nonturbulent portions of the atmosphere are subjected to fluctuations in shear and/or potential temperature gradient caused by gravity wave disturbances. These fluctuations may cause turbulence as described in the section on statistical

models of CAT. Synoptic and mesoscale dynamical processes also cause evolutions in the shear and lapse rates which can cause turbulence. A classic example of this is the persistent regions of CAT found above and below well developed jet streams. If we take the vertical derivatives of the standard budget equations for the mean wind and potential temperature, then we can create budget equations for the evolution of mean shear and mean lapse rate. These can, in principle, be combined to yield a budget equation for the Richardson number- a 'Richardsonnumberogenesis' process, to paraphrase meteorological jargon.

Once a layer of thickness, H, becomes turbulent, it is of interest to ponder the temporal duration of the turbulent event. If the turbulence is caused by a gravity wave fluctuation, then we do not expect the event to last more than a fraction of an inertial period (say, a few hours). If the breakdown is due to synoptic processes, then in principle the turbulence can endure as long as the 'Richardsonnumberogenesis' can maintain the instability against turbulent mixing. Once a layer is turbulent, the mixing process tends to cause Ri to increase. This is because $\partial U/\partial z$ an $\partial \theta/\partial z$ are both reduced by mixing, but $\partial U/\partial z$ occurs as the inverse square in Ri. Thus, we anticipate that the mixing caused by the turbulence forces Ri to increase until Ri≃1. At this point, shear production of TKE is roughly canceled by buoyant destruction and the turbulence begins to decay due to dissipation. This process occurs long before we reach ϵ_t. In other words, shear production is still active, the fluxes are still nonzero, but buoyant destruction and dissipation exceed production. The layer is decaying but it is still active.

This suggests that we must consider two more time scales: the time scale for the mixing process to occur, τ_m, and the time scale for the active region to decay to ϵ_t. We assume that the mixing process must transform

kinetic energy into potential energy by destroying the ambient potential temperature gradient for a layer of thickness. Gregg (1987) has shown that this requires an amount to energy equal to $(1/12)N^2H^2$, where N is computed from the background lapse rate when turbulent breakdown occurs. Suppose we let P be the shear production of TKE and B the buoyant destruction integrated of the entire thickness of the layer (thus, transport terms become zero); then in a state of slowly evolving equilibrium, the TKE budget equation implies the balance

$$P = B + \epsilon \tag{27}$$

If we substitute the flux Richardson number, Rf=P/B, we get a relation for the mixing time constant

$$\epsilon\tau_m = (1/Rf-1)B\tau_m = (1/Rf-1)N^2H^2/12 = [(Pr-Ri)/Ri]\ N^2H^2/12 \tag{28}$$

Therefore, we can write τ_m as

$$\tau_m = N^2H^2/(12\ \epsilon\ \gamma) \tag{29}$$

Aircraft measurements of the covariance and gradient terms (Kennedy and Shapiro; 1975, 1980) in the vicinity of the jet stream give an average value of $\gamma \simeq 0.40$. Representative values in (29) give τ_m on the order of 1 hour for a 100 m thick layer with $\epsilon = 1*10^{-4}\ m^2s^{-3}$. Notice that (29) implies that thicker layers and weaker layers (ϵ smaller) will persist much longer.

Once the layer has been mixed as discussed above, then the turbulence begins to decay with the time constant t_o described in III-D. According to

(25), even if t_o is relatively short (a few tens of minutes), it will still take hours for ϵ to decay from 10^{-4} to the transition level of $5*10^{-8}$.

IV. Applications of VHF and UHF Radar

The use of radar data in optical propagation and CAT studies requires consideration of several factors: radar resolution, range and measured variables, the relationship ot radar and optical parameters, and the types of studies that are appropriate for these systems. Details are provided in the literature (e.g., Hocking, 1982) and in our previous proposal, but a brief summary of the main points will be presented here.

The 50 MHz radars have vertical range gate resolution of 300 m up to 8 km and 900 m resolution up to 18 km. The high resolution mode requires 90 s to obtain one profile, the low resolution 3 minutes. In normal operations, a pair of resolution profiles is obtained in 5 minutes. The UHF radar has 100 m resolution to 2.6 km, 300 m resolution to 8 km, and 900 m resolution to 12 km. Both systems have two horizontal and one vertical beam.

The basic raw data produced by the radar is the mean Doppler shift (which is used to compute the mean wind vector), the width of the Doppler spectrum (which is related to the turbulence associated with the wind variance or the mean shear and can be used to estimate ϵ), and the backscatter intensity of the signal (which is related to the radar cross section and is used to calculate radar C_n^2). Details concerning the computation of C_n^2 from the radar signal are discussed in Appendix B. Thus the radar provides quantitative measurements of the profiles of U, $\partial U/\partial z$, σ_u, σ_w, and C_n^2. Models can be applied to this data to estimate ϵ (e.g., equation 13), K (e.g., equation 10), and even $\partial\theta/\partial z$.

The radars normally operate continuously and archive data in one hour average blocks. For intensive experiments, we archive the high resolution (temporally and spatially) data, including the raw Doppler spectra and all moment tables. An example of a time series of C_n^2 from two range gates of

a VHF system is shown in Fig. 1. A few examples of studies ideally suited to these systems are: vertical distribution of C_n^2 'hot spots', comparison of daytime versus nighttime C_n^2 at different times of the year, coincidence of high turbulence levels and wind shear/jet stream regions, and correlation with synoptic regimes.

V. Summary of Work Performed

A. Background

This project is concerned with the relationship of meteorological conditions to parameters and processes that influence the optical propagation properties of the turbulent atmosphere. The approach is centered around the establishment of a climatology of refractive index structure function parameter as measured with a network of Doppler radars. The relation of the atmospheric turbulence profile to the synoptic context and a model to predict the profile using standard meteorological profile data is also being investigated. The study features two modes of data archiving: (1) continuous archiving of 1 hr average wind profiles and turbulence levels, and (2) high time resolution measurements in association with other measurements (ground-based optical scintillometers, aircraft or radiosondes) in an intensive 'campaign' given the acronym EWAK.

This project funded one graduate assistant (Syrett) who studied the correlation of turbulence with synoptic context (in relation to jet streams). Two Air Force graduate students have also been working on the project. Capt. Michael Moss is completing a Ph.D. dissertation involving radar data and the Van Zandt model and 2nd Lieut. Elizabeth Beecher has completed a comparison (M.S. thesis) of meteorological and optical microstructure from radar and in situ (particularly aircraft) measurements.

B. The EWAK Experiment

A major optical/meteorological experiment (acronamed EWAK) was held at Penn State from 15 April to 15 May, 1986. Rome Air Development Center (RADC) was planning a combined aircraft/optical experiment for the spring and we convinced them to hold the field program at PSU in order to take advantage of the radar data. Given the scale of this experiment, optical propagation

scientists from several other laboratories were also invited to participate. The enclosed table is a brief summary of the measurements and participants. All optical equipment was operated during an intensive period from 30 April to 6 May when the skies were clear on every night but one. Four aircraft flights were made (another four flights had been made earlier to calibrate the radar) and approximately 35 thermosondes were launched during this period. High time resolution data were logged on the VHF radar and the sodar was operated continuously during the optical measurements. Synoptic meteorological information was carefully analyzed and archived. A meeting was held at AFGL in early September to discuss the preliminary results. One of the PI's (CWF) and three graduate students attended and made presentations.

The standard radar equation is used to calculate C_n^2 from the received power. The calibration factor for the radar is a combination of a number of system constants: antenna gain, line loss, receiver noise, etc. However, the antenna gain for the colinear-coaxial phased arrays used with the Doppler radars has never been rigorously measured. Thus, even the most careful determination of the other calibration factors cannot eliminate all of the uncertainty. Because of this, since the Penn State radars are modeled after the NOAA/WPL systems, we initially decided to use the system constants from the NOAA radars. The analysis of the EWAK data is still ongoing, but it has revealed that the radar calibration is quite good; the values of C_n^2 need to be increased by about a factor of two to agree with the thermosonde balloon measurements. A sample comparison of the uncorrected radar, thermosonde and aircraft profiles of optical C_n^2 is shown in Fig. 2.

Summary of measurements for the EWAK experiment.

Measurement	Institution	Contact
Surface micromet	PSU	C.Fairall
Sodar	PSU	D.Thomson
VHF1,VHF2	PSU	D.Thomson
Thermosonde (Cn^2)	AFGL	J.Brown
Aircraft	ARA	R.Markson
Optical Cn^2 profile#1	RADC	D.Stebbins
Optical Cn^2 profile#2	AFGL	E.Murphy
Optical scintillometer(r0)	NPS	D.Walters
Optical isoplanometer	AFWL	J.Davidson

Analysis of the aircraft data has been completed and published initially in December (Beecher, 1987) in the form of an M.S. thesis. An initial scientific publication has also been completed (Fairall et al., 1988). We will present a few examples from this work. Fig. 3 shows a sample aircraft profile of microturbulence data from one of the eight flights made during EWAK. Fig. 4 shows two comparisons of optical C_n^2 obtained from the aircraft, the thermosonde, the radar, the Van Zandt model and optical scintillometer data. The optical data is highly variable over the one hour period but is in agreement with the thermosonde and clearly lower than the other two independent methods. Finally, a conglomerate analysis of the small scale turbulence from all flights is shown in Fig. 5. Here the relation of thermal and velocity microstructure (as in equation 13) is examined. Notice that for the special case of temperature

$$(\partial X/\partial z)^2/N^2 = (T/g)\ \partial\theta/\partial z \qquad (30)$$

By plotting C_T^2 versus $(T/g)\ \partial\theta/\partial z\ C_u^2$ in log-log format, we expect the points to define the dependence of $\beta_\theta\gamma_\theta/\beta_u$. If γ_θ is constant, then we expect a straight line with a slope of one. Clearly this is not what we observed. For strong turbulence (clearly active and nondecaying regions with $\epsilon>10^{-4}$), the data gives a value of γ_θ of about 0.5, which is consistent with the jet stream value 0.4 of Kennedy and Shapiro (1980) and the oceanic value 0.3 of Gregg (1987). For the weaker turbulence cases, this value increases by about a factor of 10. The significance of this is not clear. Presently we are not sure of the effects of the vertical averaging necessary to produce the 300 m resolution which is required in order for the data to be compatible with that from the radar.

The second part of the EWAK study is an in depth investigation of the radar C_n^2 and wind data for the EWAK period by Mike Moss, an Air Force graduate student enrolled at Florida State University. This work involves the Van Zandt model, the thermosondes, and the optical data. Since this is a Ph.D. thesis project (which requires three or four years of work), we do not anticipate final results until next year. A preliminary description of the work in progress has been prepared (Moss, 1986).

C. Climatological/Synoptic Studies

The initial steps in the climatological study of the synoptic context of C_n^2 have been completed. We have been routinely archiving winds and power at one hour intervals. During a one year period, each hour was assigned a synoptic classification based on the weather charts. A grand ensemble analysis of this data base has not been started. For the purposes of this project, we have completed a detailed analysis of one selected synoptic

feature that is of particular interest: the jet stream and the wind shear in its vicinity. This work has now been published initially in the form of an M.S. thesis (Syrett, 1987). A scientific publication is now in preparation (Syrett and Thomson, 1988). Another phase of this work involves comparison of the radar measured winds with both analyzed and predicted winds for the NWS Nested Grid Model (NGM). A paper on this topic has been presented (Thomson et al., 1988). This work is relevant to the numerical prediction of C_n^2 from NGM products.

Hourly measurements of wind speed and direction were examined for two prolonged jet stream occurrences over western Pennsylvania. Data from two of the Penn State radars (McElevys Fort and Crown) were stratified into categories based on location of the jet axis relative to the site. Low resolution data from the Crown radar were also compared to the Pittsburgh rawinsonde. Potential temperature profiles were obtained using isentropically interpolated T and T_d soundings. The combination of measured wind and interpolated temperature profiles allowed low resolution Ri profiles to be generated for the profiler sounding volume. Both Ri and wind shear statistics were examined along with pilot reports of turbulence in the vicinity of the profiler.

Two cases were examined. Case 1 lasted from 7 November to 14 November 1986. Jet stream case 2 lasted from January 15 to January 23, 1987. A sample time-height cross section of wind speed (Fig. 6) illustrates the structure and variability of the jet stream at the Crown site (just north of Cook Forest in western Pennsylvania). The data were separated into five position categories. The average wind speed and Ri profiles for case 2 are shown in Fig. 7. The vertical resolution of the profiler data is slightly less than 1 km, but was interpolated to 250 m resolution for the analysis. The potential temperature

profiles also have low horizontal resolution because they are extracted from smoothed fields from the NWS observing network. Notice the minima in Ri in the regions of maximum shear above and below the peak of the jet. Pilot reports of the altitude and severity of turbulence for the western Pennsylvania region were compiled for the period of the event (Fig. 8). The PIREPS were most closely correlated with the magnitude of the shear observed by the radar, rather than the occurrences of low values of Ri (Fig. 9). This figure unequivocally shows that regions of strong shear are almost sure to have severe turbulence. This is consistent with (19a) which implies the strongest turbulence in the thickest layers (largest L_o) and the regions of greatest wind shear ($\partial U/\partial z$). Also, recall that (29) implies that the thickest layers are also the longest lived and, therefore, the most likely to be encountered by aircraft. This result suggests that, as far as severe turbulence is concerned, it is probably a mistake to attempt to derive the Richardson number from low resolution sources, partly because regions of strong shear are likely to have small Ri anyway.

Preliminary results from the comparisons of the profiler winds with the NGM winds have been surprising. The profiler winds have been compared with analyzed (0 hour 'forecast') and predicted (48 hour forecast) NGM winds. The NGM data is interpolated to the profiler location (both Crown and McElevys Fort sites were used). The profiler data has been examined with several time resolutions: the basic one hour average at the time of the NGM data, a seven hour average (plus and minus three hours about the time of the observation), and a thirteen hour average. The comparison is best for the longer time average, indicating the amount of spatial averaging inherent in the regional scale model or smoothing of extreme observations in the radar data. A sample comparison for the 500 mb wind speed and direction for May, 1987, is shown for

the analysis (Fig. 10) and the 48 hour forecast (Fig. 11). The initial analysis is typically 2.5 m/s different from the radar data and there appears to be no significant systematic bias in the wind direction. It is believed that the NGM underestimates the winds compared to the radar because of smoothing of the fields in the analysis procedure. The 48 hour forecast is noticeably more inaccurate than the analysis, but the deterioration is surprisingly small.

VI. Suggested Future Research

The general goal of this research is to investigate the fundamental relationsnips between mean atmospheric structure and microturbulence parameters such as C_n^2. We wish to study the processes that lead to temporal/horizontal variability and vertical distribution of C_n^2. The next obvious step in this investigation is to acquire and analyze data from three primary sources:

(1) Existing data. Radar data from VHF1 and VHF2 archived over the past two years will be available for completion of a climatological analysis. Raw aircraft turbulence data, which is archived on FM tapes, and raw aircraft mean profile data, which is archived on digital tapes with 2 second resolution, from the EWAK experiment could be reanalyzed with finer resolution.

(2) New Profiler data. We will continue to archive one hour average radar data from VHF1, VHF2, and VHF3 (which is to be in operation in September, 1988). We will also archive one hour average data from the UHF radar, which is to begin regular operation at State College in July, 1988. Also, we hope to begin operation of the mm-wave radiometer system in State College about July of 1988. This system will archive two minute time resolution measurements of integrated water vapor/liquid and temperature profiles. The mesoscale triangle (about 140 km sides) of VHF radar combined with the UHF and thermodynamic sounders will provide an unprecedented look at atmospheric turbulence and dynamical processes.

(3) Intensive Turbulence and Optical Propagation Experiment (EWAK II). Sometime in the near future it makes sense to have another field program similar to EWAK. We would try to work with the same

institutions as before for the optical measurements. We could also try to interest and invite NASA and NOAA groups with relevant measurement systems (e.g., Melfi's raman lidar).

The variety of scientific issues of interest were discussed in section III. We can divide the issues into four general categories: spatial structure, turbulence dynamics, climatology/synoptic correlations, and comparisons of optical, radar and in situ measurements.

A. Spatial Structure

The vertical distribution of the active turbulence areas can be studied with combined aircraft and radar data. We are interested in the probability distributions of patch size, patch lifetime, turbulence scales,and the autocorrelation functions of patch distribution. We can also use aircraft measurements to examine the probability distributions of lapse rate and shear (basic parameterizations in the Van Zandt model). The horizontal and temporal persistence of individual turbulent layers can be studied by cross correlation the C_n^2 data from the three VHF radars and by examining level flight aircraft data.

B. Turbulence Dynamics

Here the emphasis is on the microturbulence scaling relations (e.g., the ratio C_T^2/C_u^2), the generation and decay process, and the turbulence size scales (L_b and L_o). Aircraft, radar and thermosonde data can all be used. We suggest investigating the use of the radar to measure ϵ from the width of the Doppler spectrum. Furthermore, we can compare ϵ derived from the width of, for example, a 300 m range resolution spectrum with that from the mean shear derived from overlapping 100 m range resolution data. Thus, we can examine simultaneous measurements of C_T^2 and C_u^2. The size scales of turbulence can be investigated in several ways. The operation of colocated

VHF and UHF radar will also provide information about the relative intensity of turbulence size scales since they scatter from different atmospheric scales ($\lambda/2 \simeq 3$ m and 0.3 m respectively). Profiles of mean temperature from aircraft, rawinsonde, thermosonde, and radiometers would give an indication of N which, combined with ϵ, gives L_b. The vertical velocity spectrum from the radar can also give an indication of size scales. In active turbulent layers it should reveal L_o; in more quiescent layers it should indicate N. In the intensive experiment, a great deal of effort could be devoted to examining these issues.

C. Climatology/Synoptic

The mesoscale triangle of VHF radar will provide high quality dynamical variables usually not available (e.g, divergence and vorticity) that will be extremely useful in interpreting variability in C_n^2. For example, the jet stream study referred to in section IV would have greatly benefited from a more quantitative classification of conditions than the crude 'distance from the jet axis' categories used. The temperature/humidity radiometers also provide very accurate estimates of dynamic height (e.g., 500 mb) to augment the radar information. We presently plan to continue the large scale synoptic classifications for the gross climatological analysis. We will also continue the studies of the comparisons of radar data and NGM analyzed and forecast fields.

D. Comparison of Optical and Meteorological Sensors

We strongly recommend that another joint meteorological and optical experiment be held a Penn State. EWAK I revealed that there are still substantial differences between the various observing systems (often an order of magnitude). Some of this is due to differences in temporal and spatial averaging techniques but a great deal of the disagreement must be due to

undiagnosed problems with the sensors and data processing. A new intensive program would also provide us with other sources of data (e.g., thermosondes and aircraft) and much better spatial and temporal resolution of the important variables. This is necessary, in particular, to determine the importance of the averaging process on the interpretation of measurements and models.

VII. References

Barat, J. and F. Bertin, 1984: Simultaneous measurements of temperature and velocity fluctuations within clear air turbulence layers: Analysis of the estimate of dissipation rate by remote sensing techniques. J. Atmos. Sci., 41, 1613-1619.

Beecher, E.A., 1987: Analysis of temperature and velocity microturbulence parameters from aircraft data and relation to atmospheric refraction index structure. M.S. thesis, Pennsylvania State University, pp165.

Carlson, C.A., 1987: Kinematic quantities derived from a triangle of VHF Doppler wind profilers. M.S. thesis, Pennsylvania State University.

Dillon, T.M., 1982: Vertical overturns: A comparison of Thorpe and Ozmidov length scales. J. Geophys. Res., 87, 9601-9613.

Fairall, C.W., K.L. Davidson and G.E. Schacher, 1982: Meteorological models for optical properties in the marine atmospheric boundary layer. Opt. Engineer., 21, 847-857.

Fairall, C.W. and R. Markson, 1984: Aircraft measurements of temperature and velocity microturbulence in the stably stratified free troposphere. Proc. Seventh Symposium on Turbulence and Diffusion, AMS, Boulder, CO.

Fairall, C.W., 1987: A top-down and bottom-up diffusion model of C_T^2 and C_q^2 in the entraining convective boundary layer. J. Atmos. Sci., 44, 1009-1017.

Fairall, C.W., D.W. Thomson, and R. Markson, 1988: An aircraft and radar study of temperature and velocity microturbulence in the stably stratified free troposphere. Proc. Eighth Symposium on Turbulence and Diffusion, AMS, San Diego, CA, 61-65.

Fried, D.L., 1966: Optical resolution through a randomly inhomogeneous medium for very long and very short exposures. J. Opt. Soc. Am., 56, 1372-1380.

Fried, D.L., 1981: Anisoplanatism in adaptive optics. Proc. AGARD Conf.#300, 'Special Topics in Optical Propagation', Monterey, CA.

Fried, D.L., and R.A. Smeltzer, 1967: Effect of atmospheric scintillation on optical data channel--laser radar and binary communications. Appl. Opt., 6, 1729-1740.

Gage, K.S., J.L. Green, and T.E. Van Zandt, 1980: Use of Doppler radar for the measurement of atmospheric turbulence parameters from the intensity of clear air echoes. Rad. Sci., 15, 407-416.

Gage, K.S. and G.D. Nastrom, 1986: Theoretical interpretation of atmospheric wavenumber spectra of wind and temperature observer by commercial aircraft during GASP. J. Atmos. Sci., 43, 729-740.

Gibson, C.H., 1987: Fossil turbulence and intermittency in sampling oceanic mixing processes. J. Geophys. Res., 92, 5383-5404.

Gossard, E.E. and A.S. Frisch, 1987: The relationship of the variance of temperature and velocity to atmospheric static stability--application to radar and acoustic sounding. J. Clim. Appl. Met., to appear.

Gregg, M.C., 1987: Diapycnal mixing in the thermocline: a review. J. Geophys. Res., 92, 5249-5286.

Hill, R.J. and S.F. Clifford, 1978: Modified spectrum of atmospheric temperature fluctuations and its application to optical propagation. J. Opt. Soc. Am., 68, 892-899.

Hocking, W.K., 1983: The relationship between strength of turbulence and backscattered radar power at HF and VHF. Proc. workshop on Technical Aspects of MST Radar, MAP Handbook #9, Urbana, Ill.

Itsweire, E.C., K.N. Helland, and C.W. Van Atta, 1986: The evolution of grid generated turbulence in a stably stratified fluid. J. Fluid. Mech., 162, 299-338.

Kennedy, P.J. and M.A. Shapiro, 1975: The energy budget in a clear air turbulence zone as observed by aircraft. Mon. Wea. Rev., 103, 650-654.

Kennedy, P.J. and M.A. Shapiro, 1980: further encounters with clear air turbulence in research aircraft. J. Atmos. Sci., 37, 986-993.

Knowlton, L.W., 1987: Kinematic diagnoses of frontal structure and circulations derived from two and three-station VHF Doppler wind profilers networks. M.S. thesis, Pennsylvania State University.

Livingston, P.M., 1972: A study of target edge response viewed through atmospheric turbulence over water. Appl. Opt., 11, 2352-2357.

Moss, M.T., 1986: Measurement and modeling of tropospheric/stratospheric refractive index structure parameter. PhD thesis prospectus, Florida State University.

Nastrom, G.D., B.B. Balsley , and K.S. gage, 1981: Change with season of C_n^2 at Poker Flat, Alaska, from MST Doppler radar observations. Proc. 20th Conf. on Radar Meteorology, AMS, Boston, MA.

Neiman, P.J., 1987: Wind profiler derived temperature gradients and advections, M.S. thesis, Pennsylvania State University.

Nieuwstadt, F.T.M., and R.A. Brost, 1986: The decay of convective turbulence. J. Atmos. Sci., 43, 532-546.

Syrett, W.J., 1987: Some applications of 50 MHz wind profiler data: detailed observations of the jet stream. M.S. thesis, Pennsylvania State University, pp135.

Syrett, W.J. and D.W. Thomson, 1988: Detailed observations of the jet stream with the Penn State VHF Doppler radar. J. Clim. Appl. Met., in preparation.

Tatarski, V.I., 1961: Wave Propagation in a Turbulent Medium, McGraw-Hill, New York, Chapter 7.

Thomson, D.W., W.J. Syrett, T.T. Warner, and N.L. Seaman, 1988: Comparisons of wind Profiler measurements with NMC NGM analyses and predictions. Proc. 8th Conf. on Numerical Weather Prediction, AMS, Feb. 22-25, Baltimore, MD, pp6.

Van Zandt, T.W., J.L. Green, K.S. Gage, and W.L. Clark, 1978: Vertical profiles of refractivity turbulence structure constant: comparison of observations by the sunset radar with a new model. Radio Sci., 5, 819-829.

Van Zandt, T.W., K.S. Gage and J.M. Warnock, 1981: An improved model for the calculation of profiles of C_n^2 and ϵ in the free atmosphere form background profiles of wind, temperature and humidity. Proc. 20th Conf. on Radar Meteorology, AMS, Boston, MA.

Wesely, M.L., 1976: The combined effect of temperature and humidity fluctuations on refractive index. J. Appl. Meteor., 15, 43-49.

VIII. Summary of Publications and Presentations

The following is a list of publications and presentations at least partially funded by or directly concerned with this research project.

A. Publications

Williams, S.R. and D.W. Thomson, 1986: An evaluation of errors observed in the measurement of low wind velocities. Handbook for MAP, Vol. 20 , SCOSTEP secretariat, Dep. Elec. Comp. Eng., Univ. IL., 256-262.

Williams, S.R., and R. Peters, 1986: The Penn State Doppler network progress report. Handbook for MAP, Vol. 20 , SCOSTEP secretariat, Dep. Elec. Comp. Eng., Univ., IL., 339-341.

Moss, M.T., 1986: Measurement and modeling of tropospheric/stratospheric refractive index structure parameter. PhD thesis prospectus, Florida State University.

Beecher, E.A., 1987: Analysis of temperature and velocity microturbulence parameters from aircraft data and relation to atmospheric refraction index structure. M.S. Thesis, Pennsylvania State University, pp165.

Syrett, W.J., 1987: Some applications of 50 MHz wind profiler data: detailed observations of the jet stream. M.S. thesis, Pennsylvania State University, pp135.

Fairall, C.W., 1987: A top-down and bottom-up diffusion model of C_T^2 and C_q^2 in the entraining convective boundary layer. J. Atmos. Sci., 44, 1009-1017.

Thomson, D.W., W.J. Syrett, T.T. Warner, and N.L. Seaman, 1988: Proc. 8th Conf. on Numerical Weather Prediction, AMS, Feb. 22-25, Baltimore, MD, pp6.

Fairall, C.W., D.W. Thomson and R. Markson, 1988: An aircraft and radar study

of temperature and velocity microturbulence in the stably stratified free troposphere. Proc. 8th Symposium on Turbulence and Diffusion, AMS, April 24-29,San Diego, CA,61-65.

Williams, S.A. and D.W. Thomson, 1988: Comparisons between Wind Profiler and conventional Loran/Omega based rawinsonde wind measurements. In preparation.

B. Oral presentations

"Clear air Doppler radar", C.W. Fairall, RISO National Laboratory (Denmark), Aug. 6, 1986.

"Turbulence measurements with Doppler profilers", D.W. Thomson, Naval Environmental Research and Prediction Facility, June 15. 1986.

"Wind and turbulence measurements with a clear air Doppler radar", C.W. Fairall, Florida State University, Aug. 28, 1986.

"An analysis of synoptic conditions during EWAK", W. Syrett, AFGL, Sept. 4, 1986.

"Radar measurements of Cn^2 during EWAK", M. Moss, AFGL, Sept. 4, 1986.

"Sodar measurements of Cn^2 during EWAK", T. Messier, AFGL, Sept. 4, 1986.

"Aircraft measurements of microturbulence during EWAK", C. Fairall, AFGL, Sept. 4, 1986.

"Wind Profilers", D.W. Thomson, a series of three lectures, Dept. of Meteorology, Naval Postgraduate School, Monterey, CA., Jan., 1987.

"Toward a physical model of C_n^2", C. Fairall, Workshop on the Physics of Directed Energy Propagation in the Atmosphere, Las Cruces, NM, March 29, 1988.

"Atmospheric radar or seeing with thick air", C.Fairall, Dept. of Physics, Naval Postgraduate School, Monterey, CA, April 20, 1988.

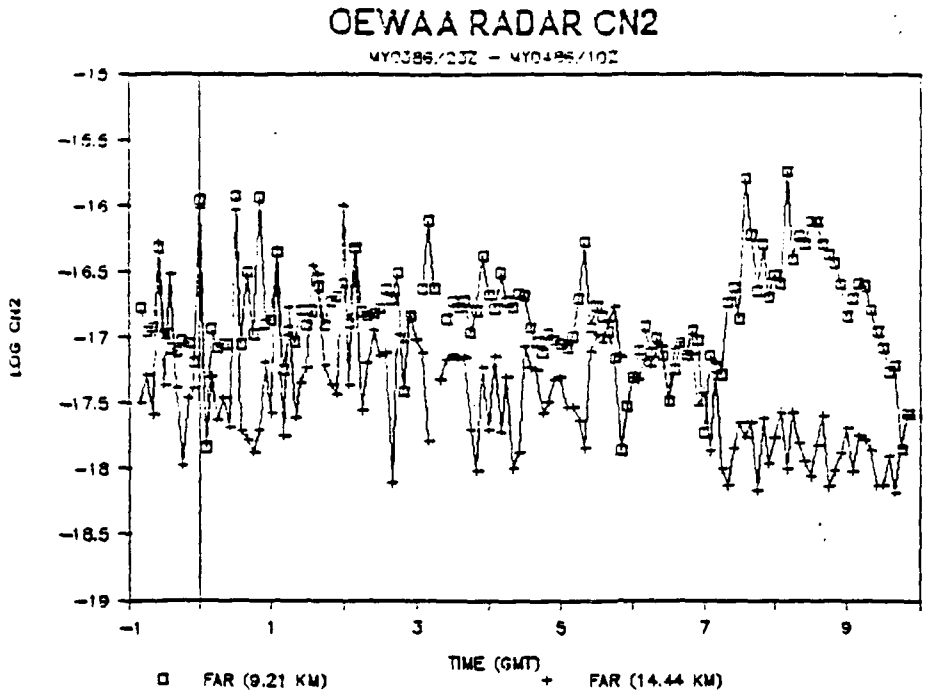

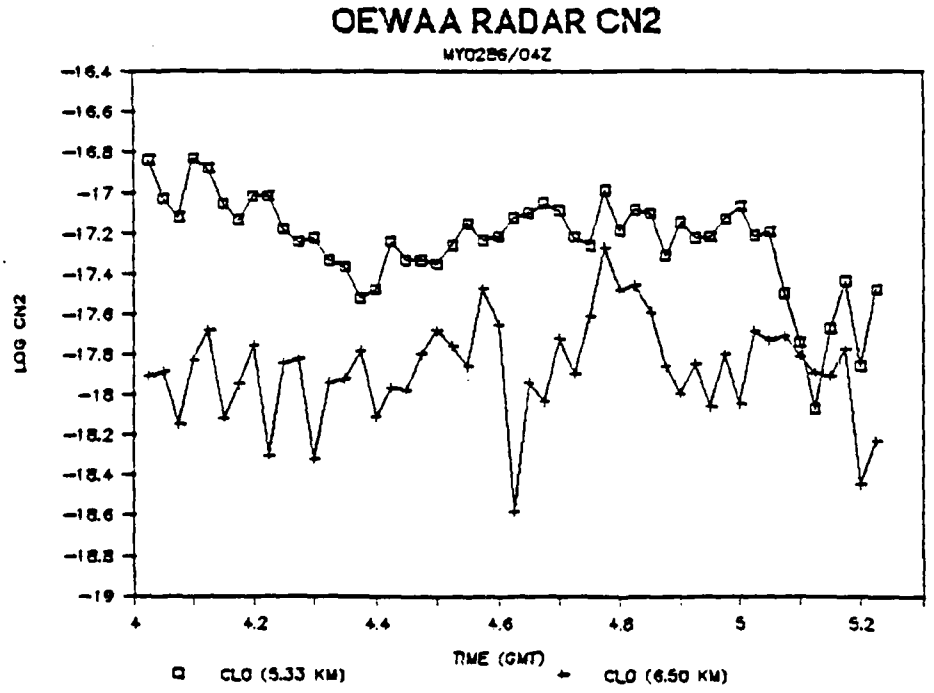

Figure 1. Sample high resolution time series of C_n^2 at two different range resolutions. The upper panel is with 0.9 km vertical resolution and 3 minute time resolution; the lower panel is with 0.3 km vertical resolution and 90 second time resolution. Each panel gives a time series for two different altitudes.

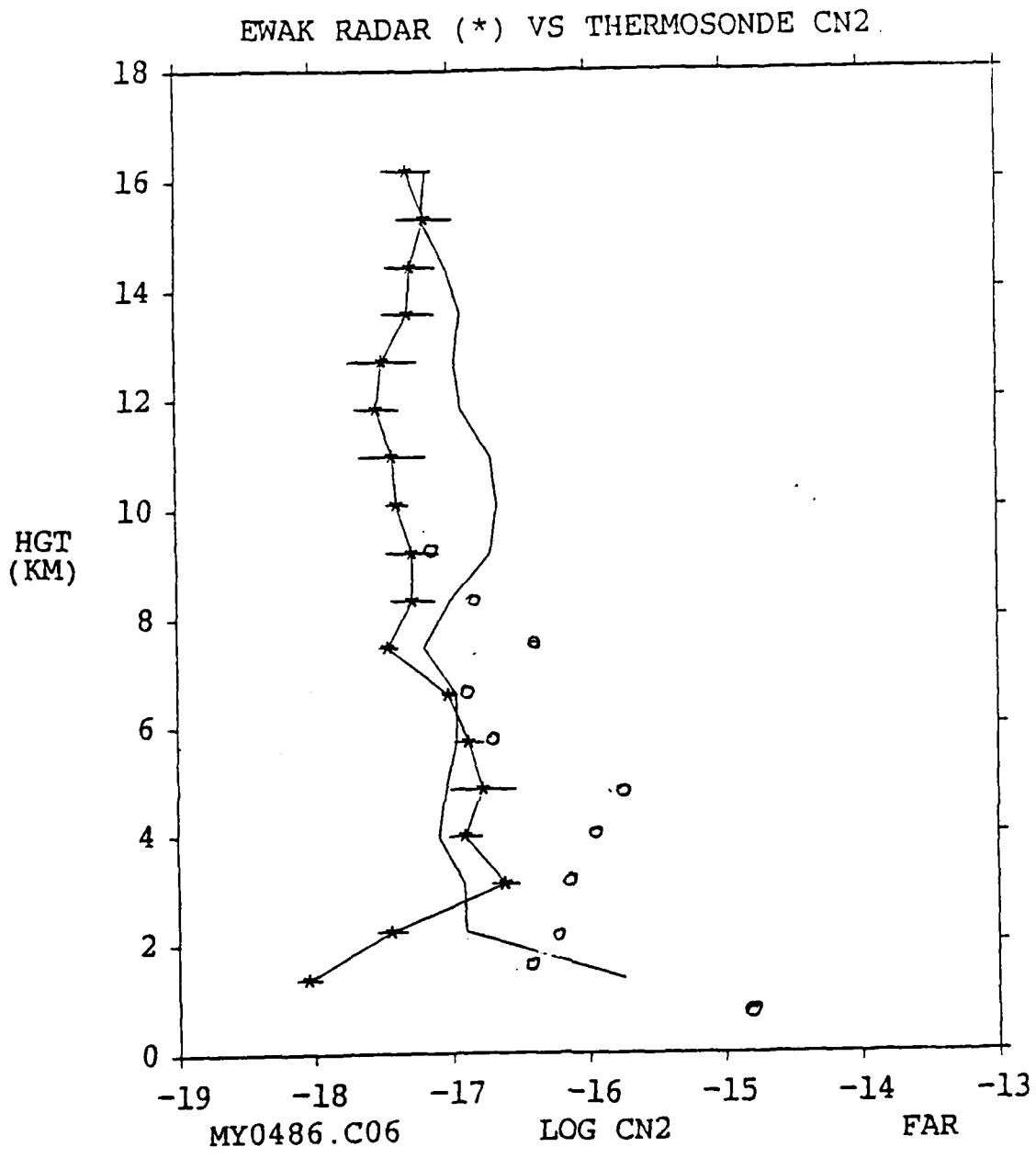

Figure 2. Sample profile of optical C_n^2 from the EWAK experiment. The * symbol denotes the radar estimate (corrected for moisture effects) with horizontal bars to indicate the standard deviation over an hour. We now believe the radar data should be increased by at least a factor of two from the values indicated in this graph. The solid line is AFGL thermosonde data degraded to the radar resolution by linear averaging. The open circles are from the aircraft measurements using the spectral method. The designator in the lower left corner indicates the profile is for May 4, 1986 at 0600 GMT.

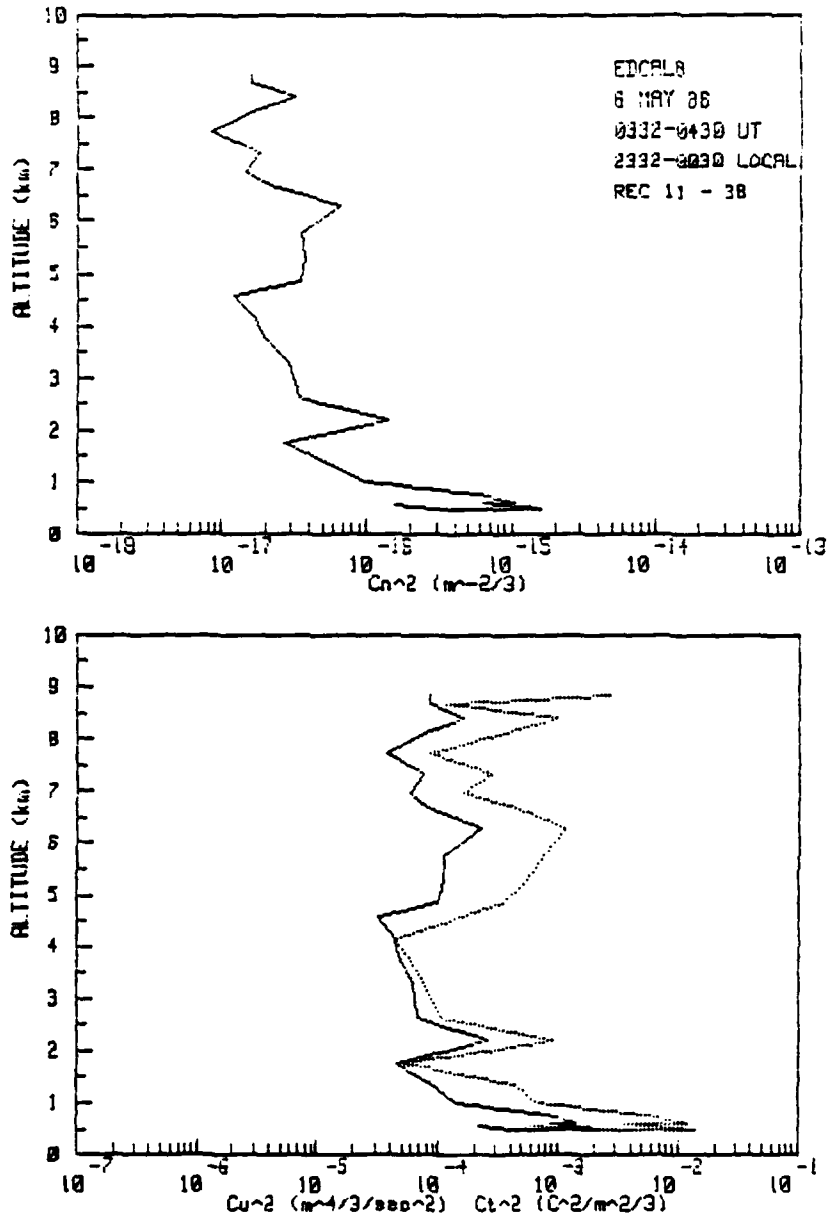

Figure 3. Sample aircraft microturbulence profile. The upper panel is optical C_n^2 vs. altitude; the lower panel is C_T^2 and C_u^2 vs. altitude.

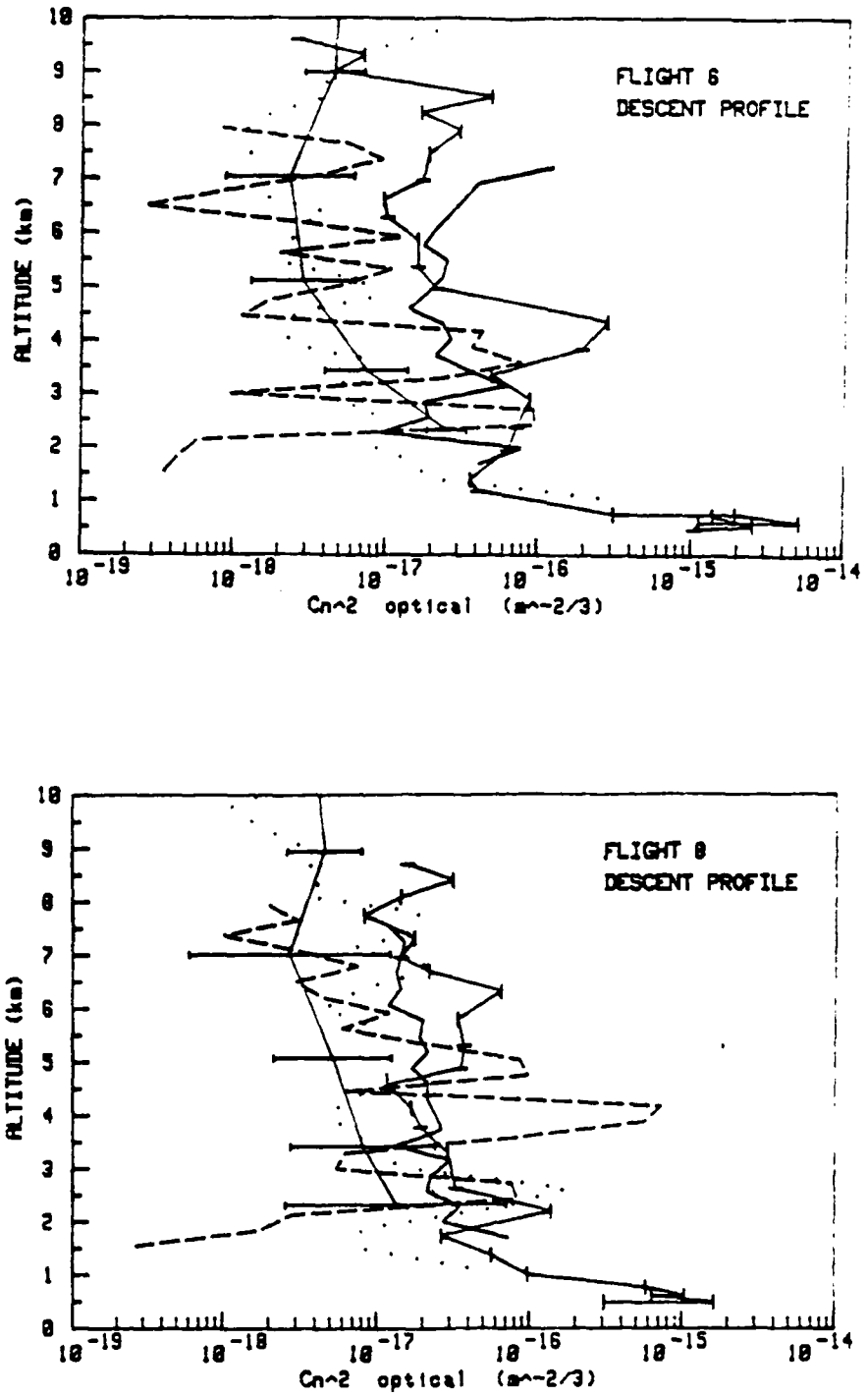

Figure 4. Comparison of various measurements of optical C_n^2 profiles from EWAK. The solid line is the Van Zandt model, the dashed line is the radar, the solid line with horizontal bars is the averaged scintillometer, the solid line with tic marks is the aircraft, and the dotted line is the thermosonde. The upper panel is at about 0000 local time on 4 May 1986; the lower panel is about 2300 local time on 5 May 1986.

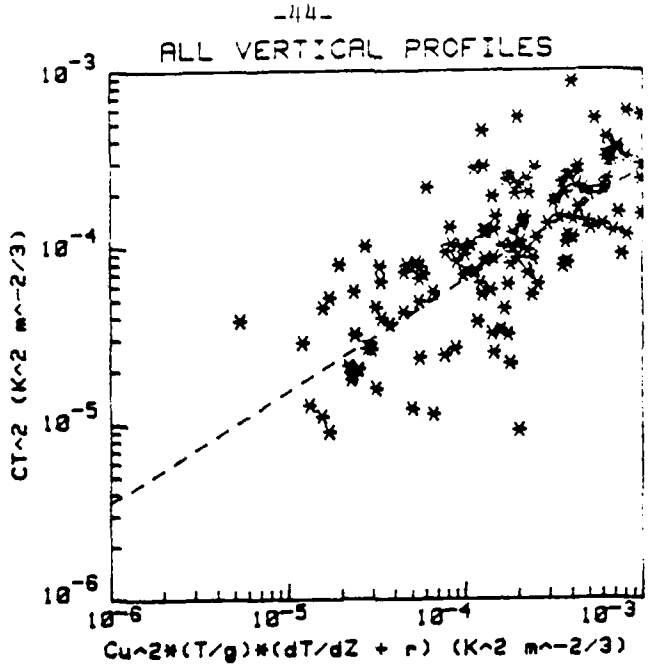

Excluding flight 6
Slope = .630
Correlation Coefficient = .797

Figure 5a. A comparison of simultaneous values of temperature and velocity microturbulence when normalized using equation 13. A slope of 1 would indicate that γ_θ was a constant.

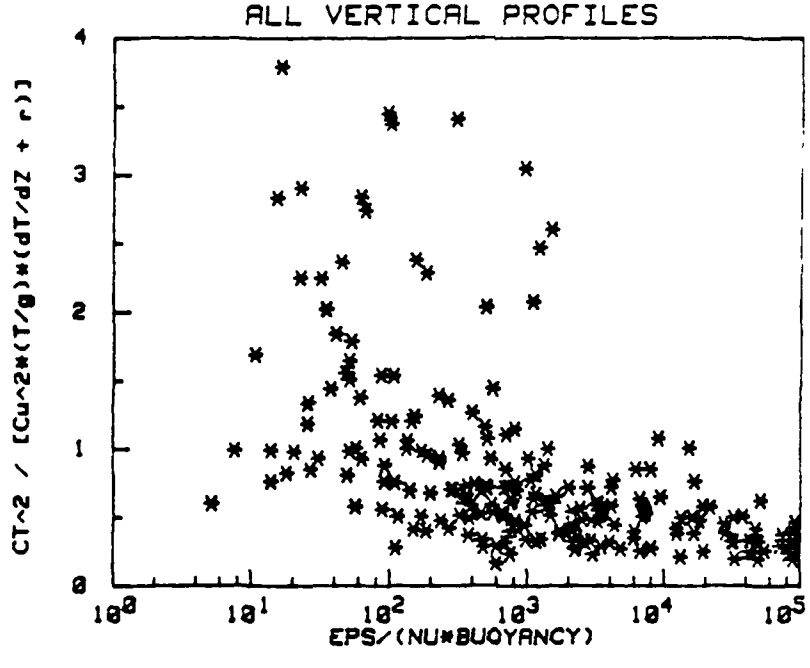

Figure 5b. A composite comparison of C_T^2 normalized by C_u^2 and potential temperature gradient (as in Eqs. 13 and 30) as a function of the activity parameter, A. A constant value would indicate that γ_θ was a constant.

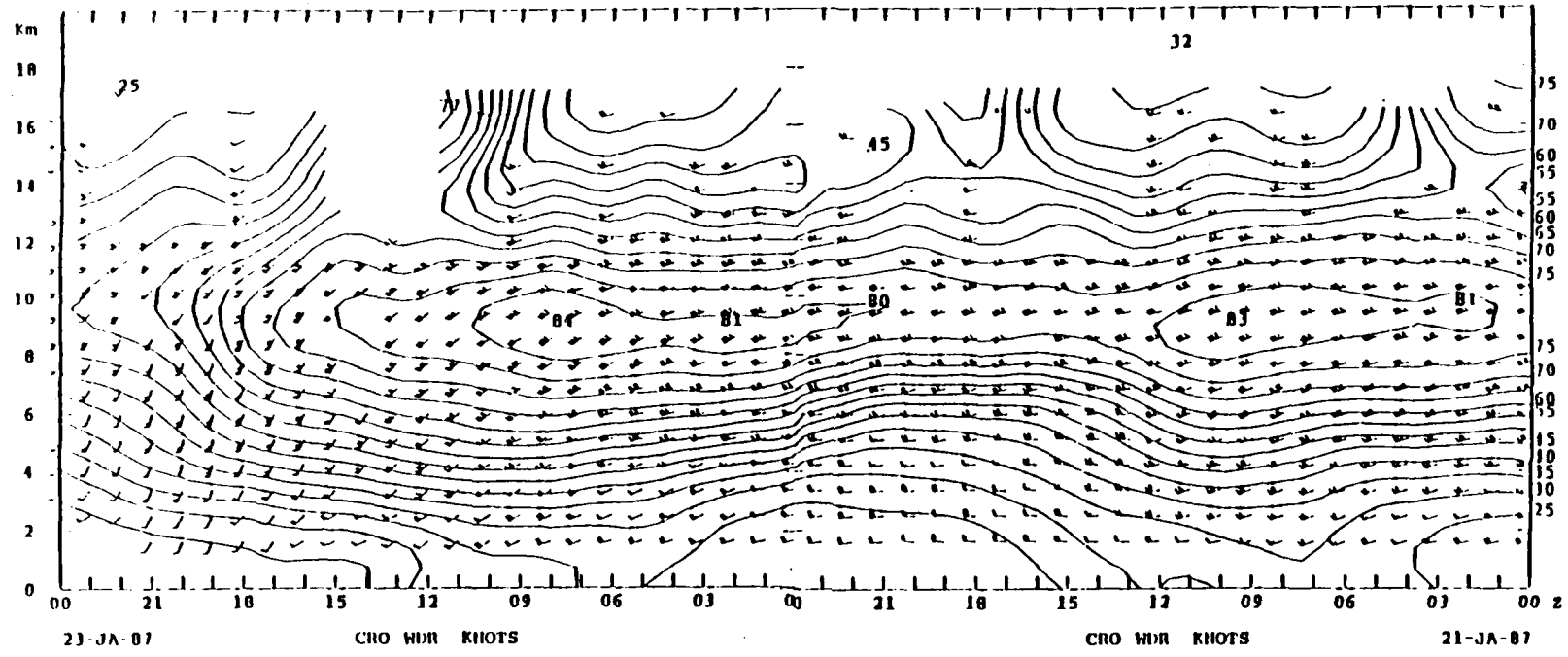

Figure 6. Time-height cross sections of radar winds and directions for a two day period (January 21, 22, 1987) from Case 2 of the study by Syrett (1987). The jet stream is apparent as the wind speed maximum at about 10 km height.

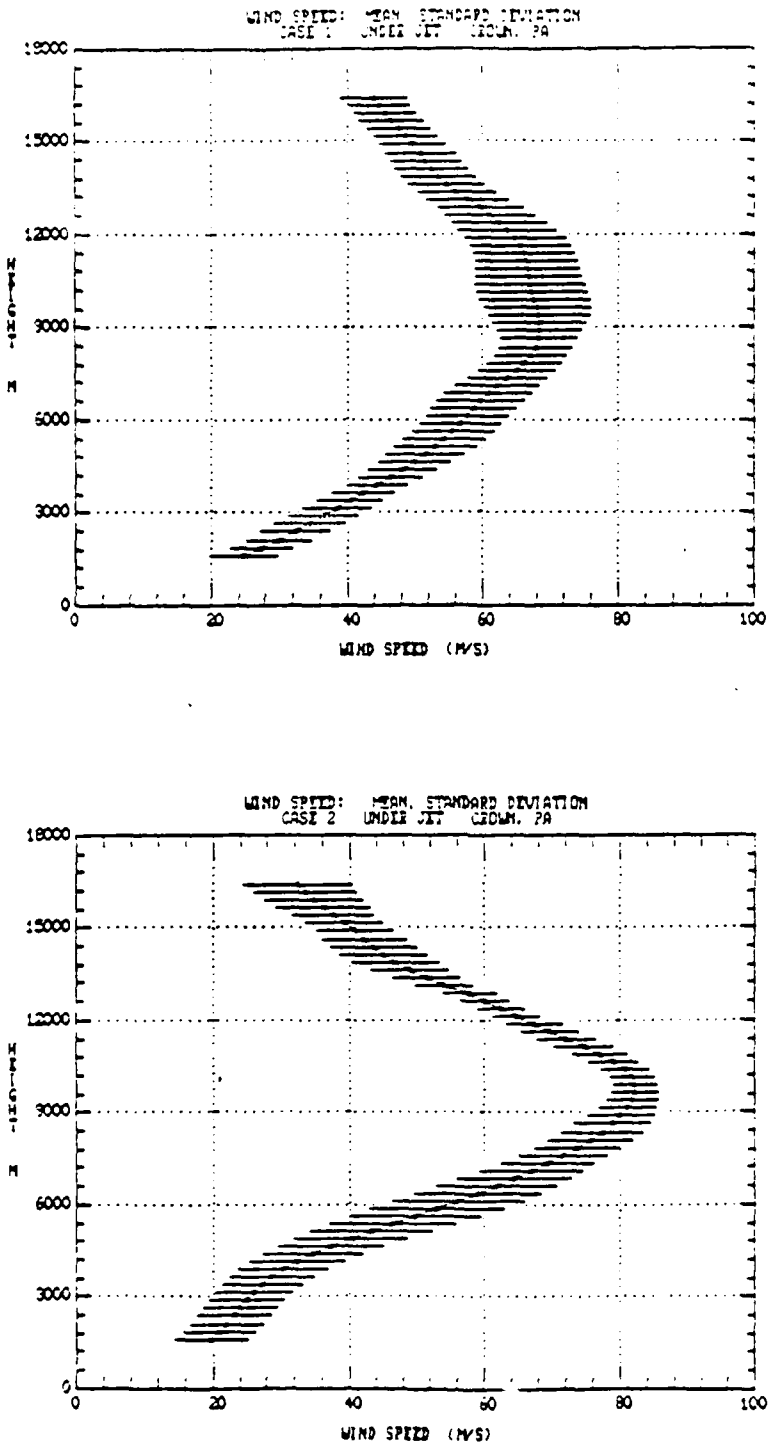

Figure 7a. Average wind speed profiles with the measurement site within 100 km of the jet axis. The horizontal bars indicate the standard deviation for the period. The upper panel is case 1; the lower panel is case 2.

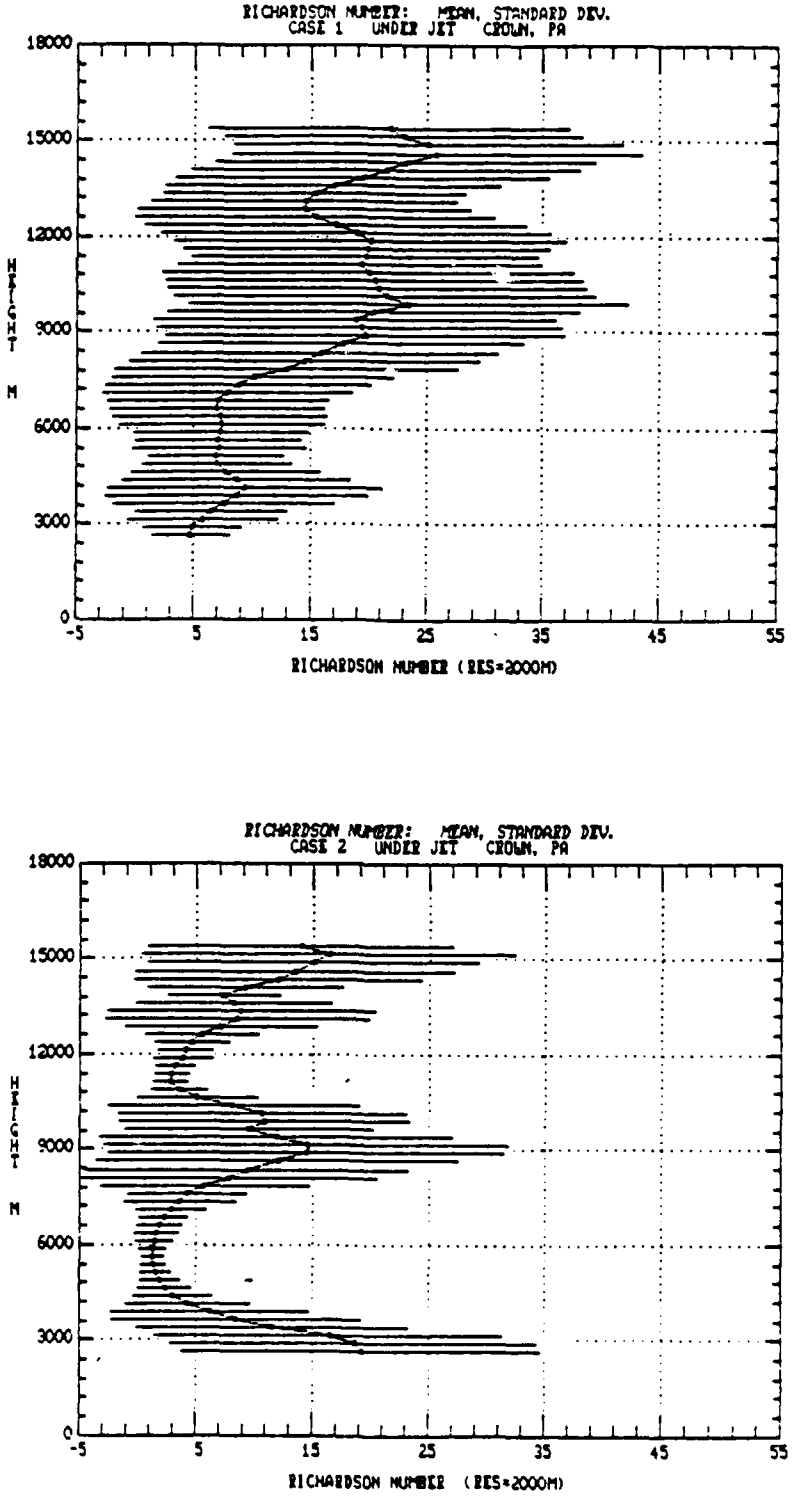

Figure 7b. As in Fig. 7a, but for the Richardson Number derived from the radar winds and interpolated rawinsonde thermodynamic data.

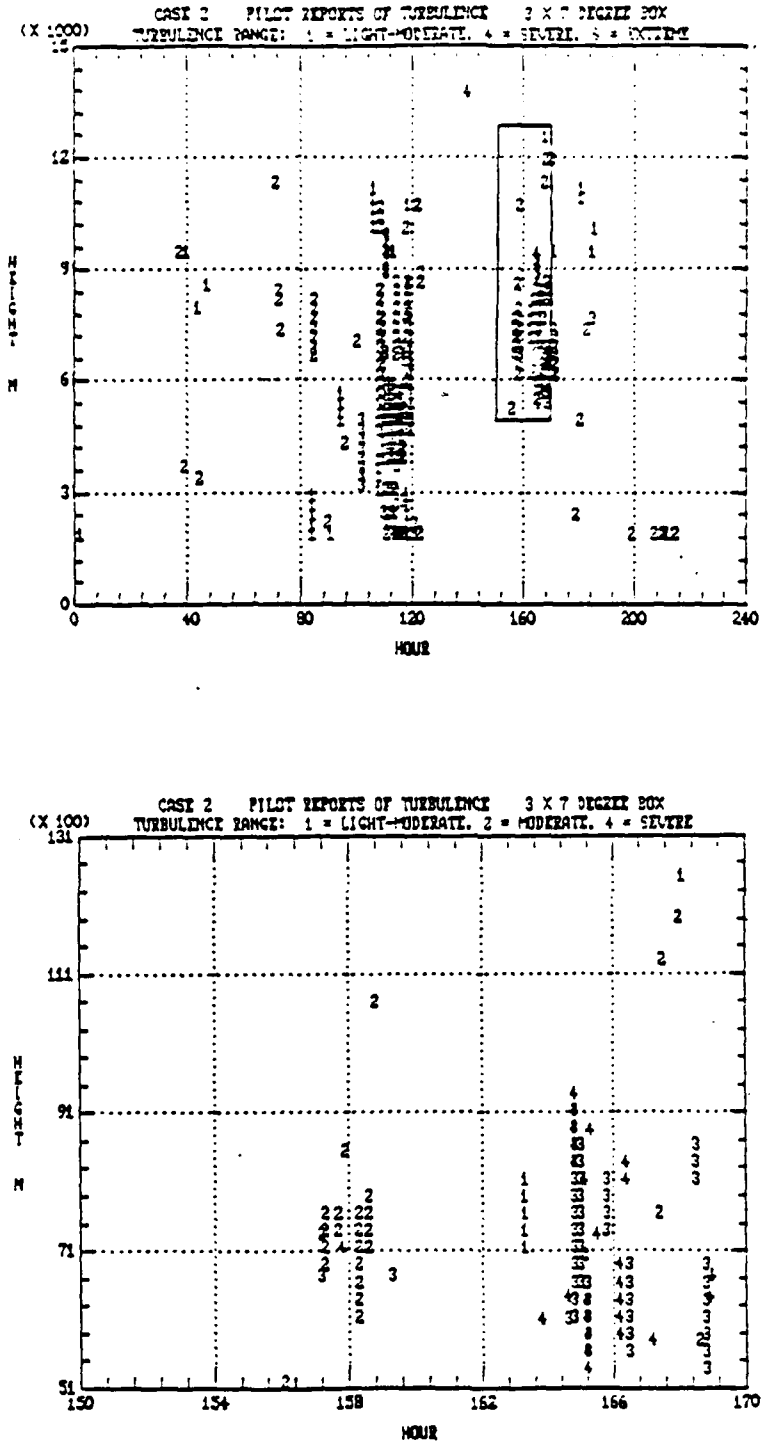

Figure 8. Pilot reports of turbulence in the vicinity of the radar during case 2. The bottom panel is a blowup of the boxed area of the top plot.

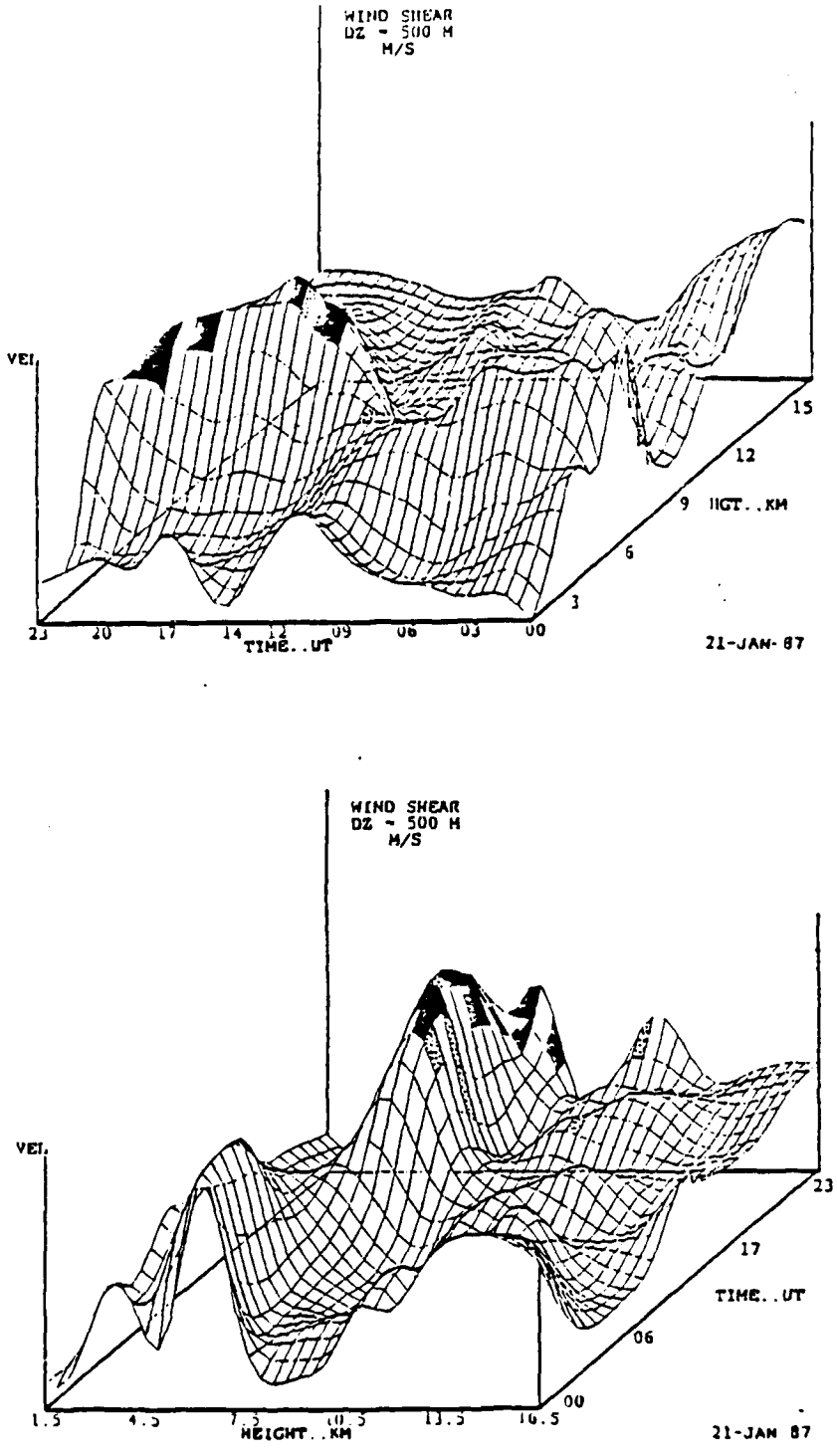

Figure 9. Surface plots of wind shear above the Crown radar during 21 January 1987. The surface defines the time, altitude and magnitude of the wind shear. The shaded areas indicate the pilot reports of turbulence: dark implies severe and dotted implies moderate. The bottom panel is a 90-degree rotation of the upper panel to provide a different view. Note that all pilot reports of severe turbulence occurred during periods of maximum wind shear.

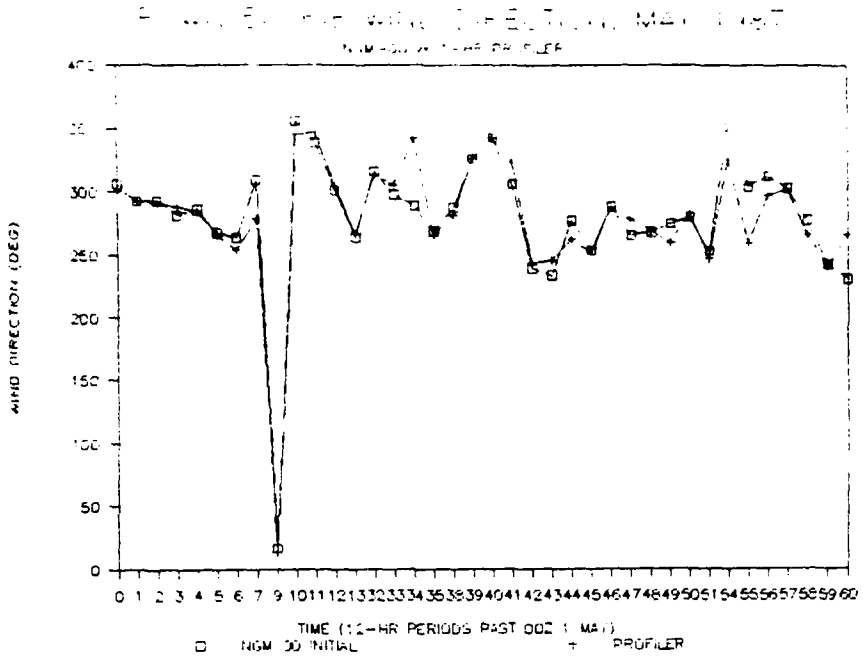

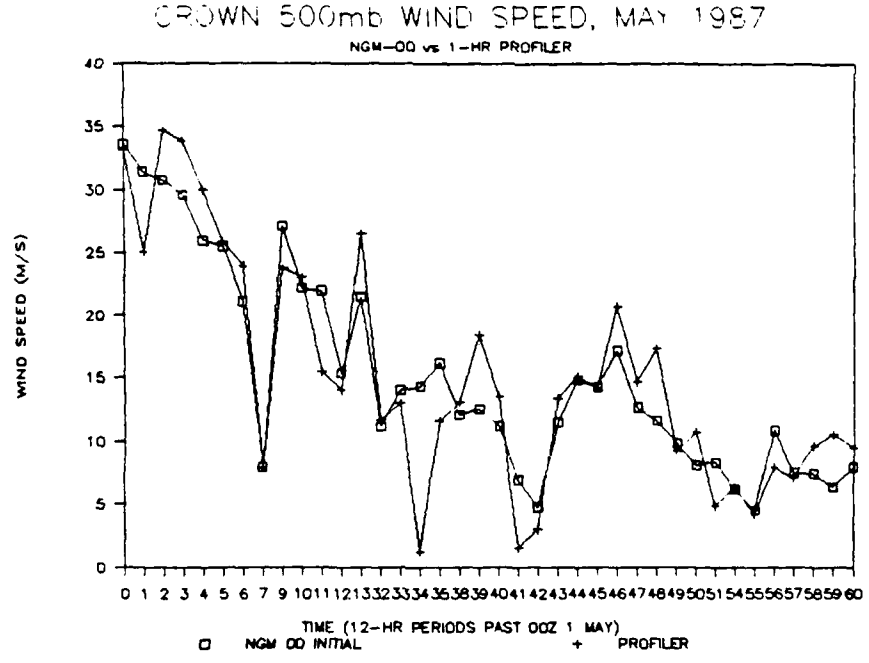

Figure 10. A comparison of the NGM interpolated and radar derived 500 mb wind direction (upper panel) and wind speed (lower panel) for the month of May, 1987. The NGM data represents the smoothed analysis field used to initialize the model (0 forecast).

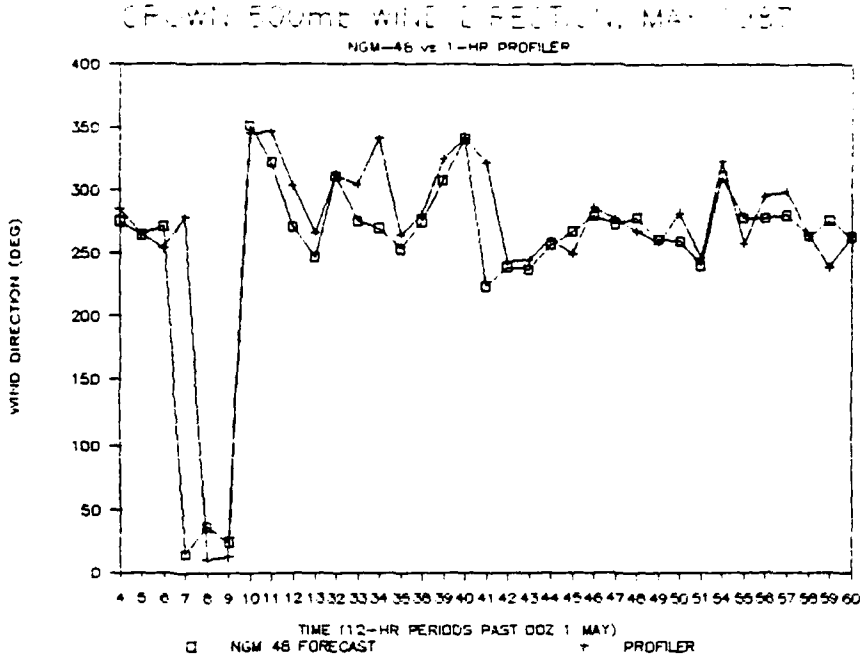

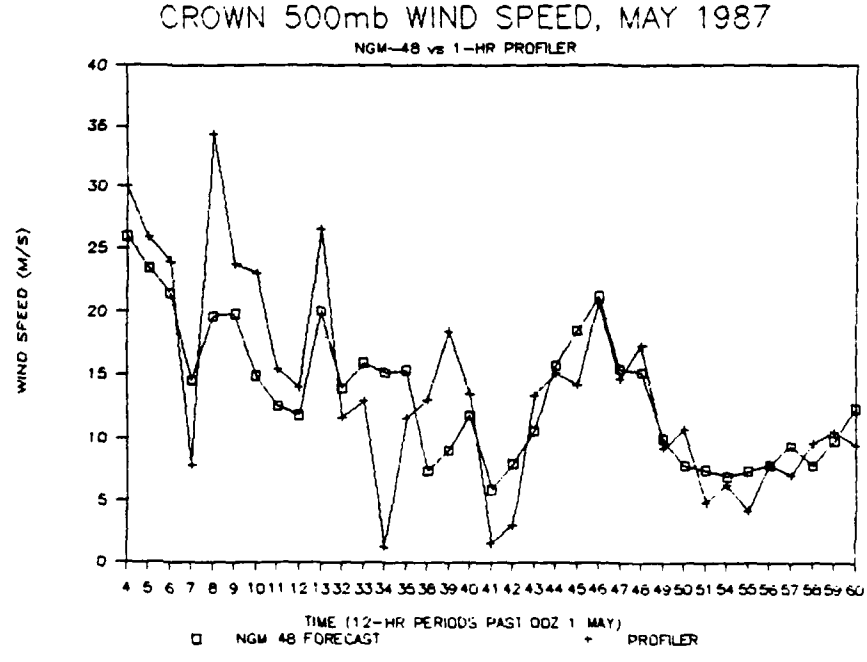

Figure 11. As in figure 10 but for the 48 hour NGM forecast.

APPENDIX A

Profiler System Description

Mesoscale meteorological measurements, analysis and prediction are some of the principal areas of research in the Department of Meteorology at Penn State. For more than a decade those members of the faculty concerned with mesoscale analysis, numerical modeling and forecasting have been frustrated by the spatial and temporal inadequacy of conventional network observations for both research and operational applications. For more than five years the Department had sought the substantial financial resources required to deploy a network of VHF Doppler (ST) radars and millimeter wave radiometers for "operational" test and evaluation for wind and thermodynamic profiling. Construction of the ST radar network began in fall of 1983 using funding provided by the Air Force Office of Scientific Research (through the DoD University Research Instrumentation Program) and the University. In 1986 a second AFOSR URIP grant was obtained to fund the acquisition of temperature (50-60 GHz) and humidity (20-30 GHz) profiling radiometers. This document will only discuss the radar systems.

For the foreseeable future the Penn State ST radar program will be focused on applications rather than systems development research. Deployment of the systems would not have been possible without the outstanding cooperation provided by C.G. Little and R. Strauch and their colleagues at the Wave Propagation Laboratory, and also J. Brosnahan of Tycho Technology from whom we bought all of the receivers, transmitters and antennas. With regard to the other major systems components, we have assembled in-house, from WPL documentation, the time-domain-integrator and computer interfaces and have purchased WPL software-compatible Data General Corp. Eclipse computers for each system.

The Penn State network consists of three 6 m wavelength(VHF) and one 0.7 m wavelength(UHF) radars. Fig. 1 indicates the approximate location of a mesoscale triangle formed by the three VHF radar sites within the routine rawinsonde network. In Table 1, a short summary of the specifications for the four radars is given. Experiences, plans and improvements for the PSU network are summarized below.

A. VHF1 50-MHz radar located 15 km south of State College, PA.

1. This system became fully operation June 27, 1985. The primary reason for system failures since the onset has been AC outages which are prevelant in this area. Battery back-up and computer-controlled autorestart of the transmitters has circumvented this problem.

2. Initial performance statistics done by Frisch et al., WPL on August 1985 data , indicate very good performance by VHF1. On Beam #1 the next to last range gate (16.8 km MSL) was able to make a wind measurement 99% of the time, while Beam #2 was able to measure the wind at this height 85% of the time. The difference between the beams is probably due to better pickup by beam #2 of computer/electronic noise from the building. Samples of data from the low altitude range of VHF1 are shown in Figs. 2 and 3.

3. A vertical beam was added in March, 1987, and the latest NOAA/WPL software was installed.

B. VHF2 50-MHz radar located in NW Pennsylvania near Crown, PA.

1. This system was installed May 1, 1986 and has operated since. Performance is often slightly better than VHF1 but a source of interference (radiotelephones from a local trucking company) leads to periods of reduced

data quality.

2. A vertical beam was added in January, 1987, and the latest NOAA/WPL software was installed.

C. VHF3 50-MHz radar located in SW Pennsylvania near Somerset, PA.

1. All hardware is ready for installation pending selection and preparation of a site.

2. A three beam system similar to VHF1 and VHF2 will be used. Some of the hardware from Tycho Technology has been slightly updated.

D. UHF1 portable 405-MHz radar to be semi-permanently based at the PSU Circleville Farm in downtown State College, PA.

1. This system has been used on three major field deployments: the SPACE/MIST-COHMEX experiment in Alabama (June-July, 1986), the FIRE stratocumulus IFO on San Nicolas Island, CA (July, 1987), and the Arizona monsoon experiment (August, 1987).

2. Preparations for basing at Circleville Farm are to be completed in July, 1988.

Table 1: Specifications for the Penn State ST Radars

Item	VHF1,VHF2,VHF3		UHF1		
Type	Pulsed Doppler, 3 beam		Pulsed Doppler, 3 beam		
Location	1: S. State College 2: Crown, PA 3: Somerset,PA		In State College, transportable		
Frequency (nom.)	49.9 MHz		404 MHz		
Bandwidth	300, 100 KHz		1, 0.3,0.07 MHz		
Peak Power	30 KW		30 KW		
Pulsewidth	3.67, 9.67 μsec		1, 4, 16 μsec		
Antenna:					
Type	Phased array CoCo		Phased array CoCo		
Dimensions	50 m X 50 m		9 m X 9 m		
Zenith angles	90°(vert),75°		90°(vert), 75°		
One site computer	Data Gen. Eclipse		Data Gen. Eclipse		
On site processing* at PW- :	3.67 μs	9.67 μs	1μs	4μs	16μs
Time domain ave	400	125	112	70	35
Spectral ave	8	16	16	32	64
Height spacing (m)	290	870	100	300	800
Spec. resolut.(m/s)	0.49	0.31	0.29	0.29	0.29
Maximum absolute rad. velocity (m/s)	15.7	19.6	18.25	18.25	18.25

*Software controllable

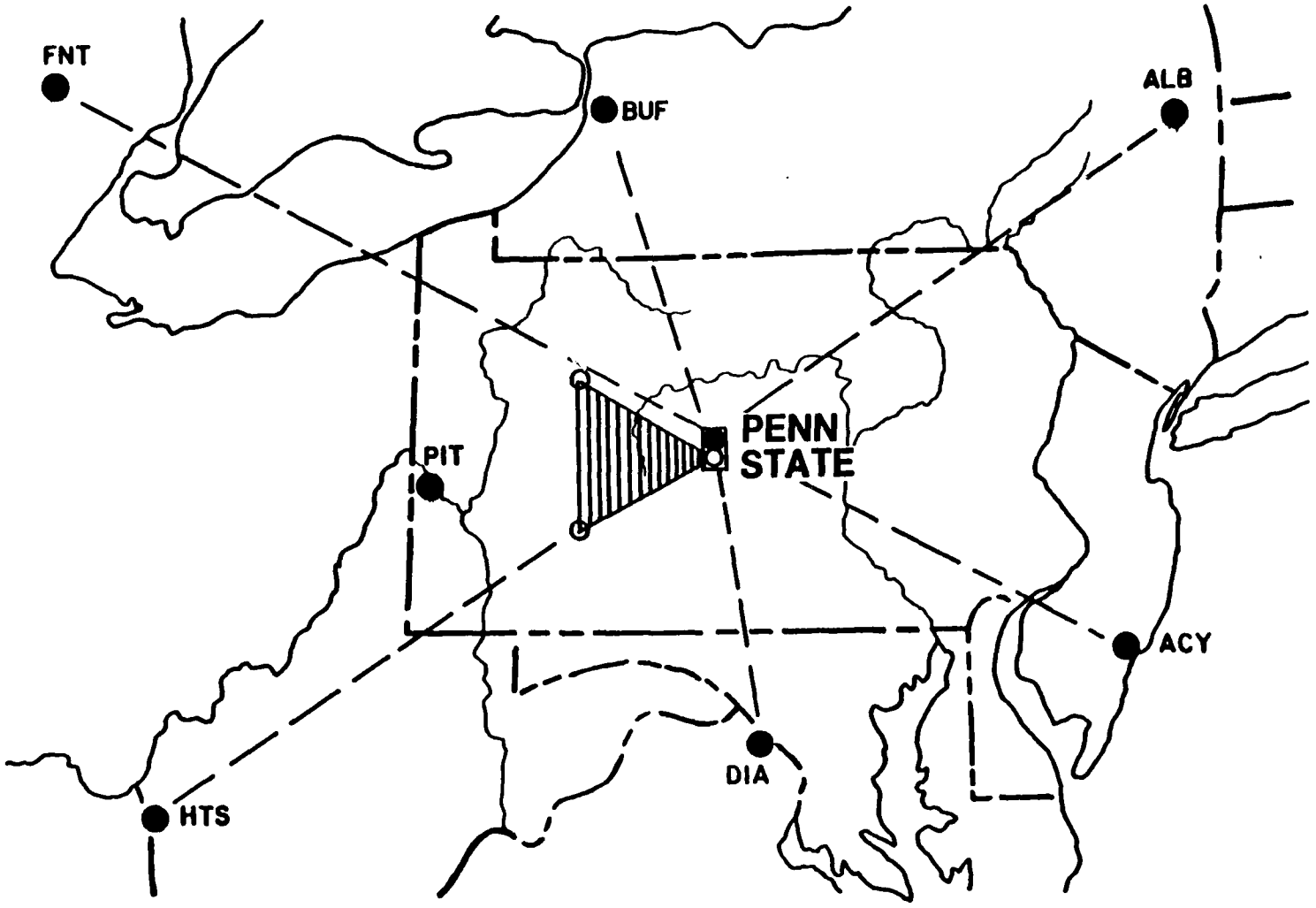

Figure 1 Locations of Penn State radar sites (open circles) and standard rawinsonde sites (solid circles).

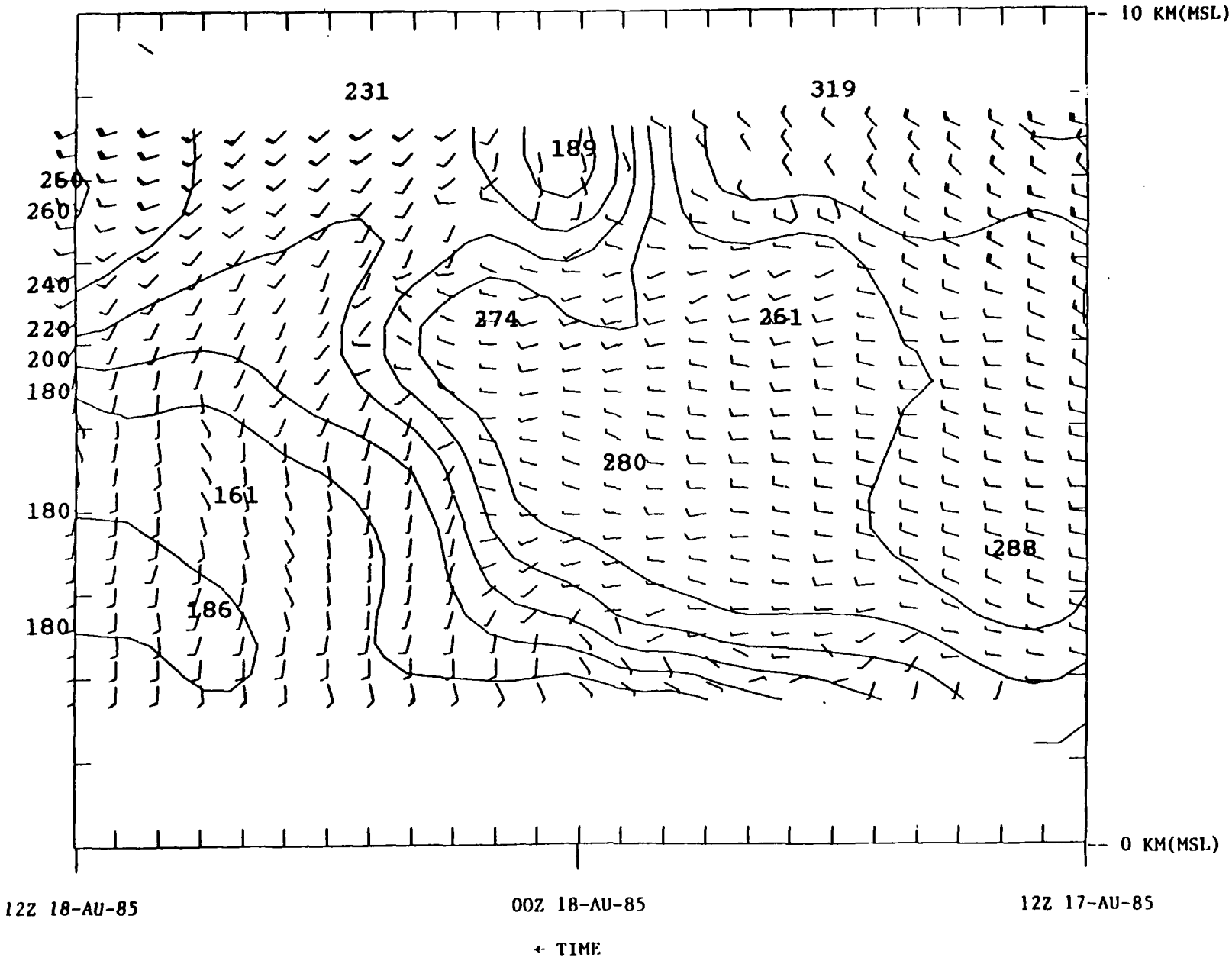

Figure 2 Time/height cross section from VHF 1 (near State College) for a 25 hour period beginning at 12Z on August 17, 1985. The arrows are standard meteorological wind barbs and the solid lines are isolines of wind direction (degrees).

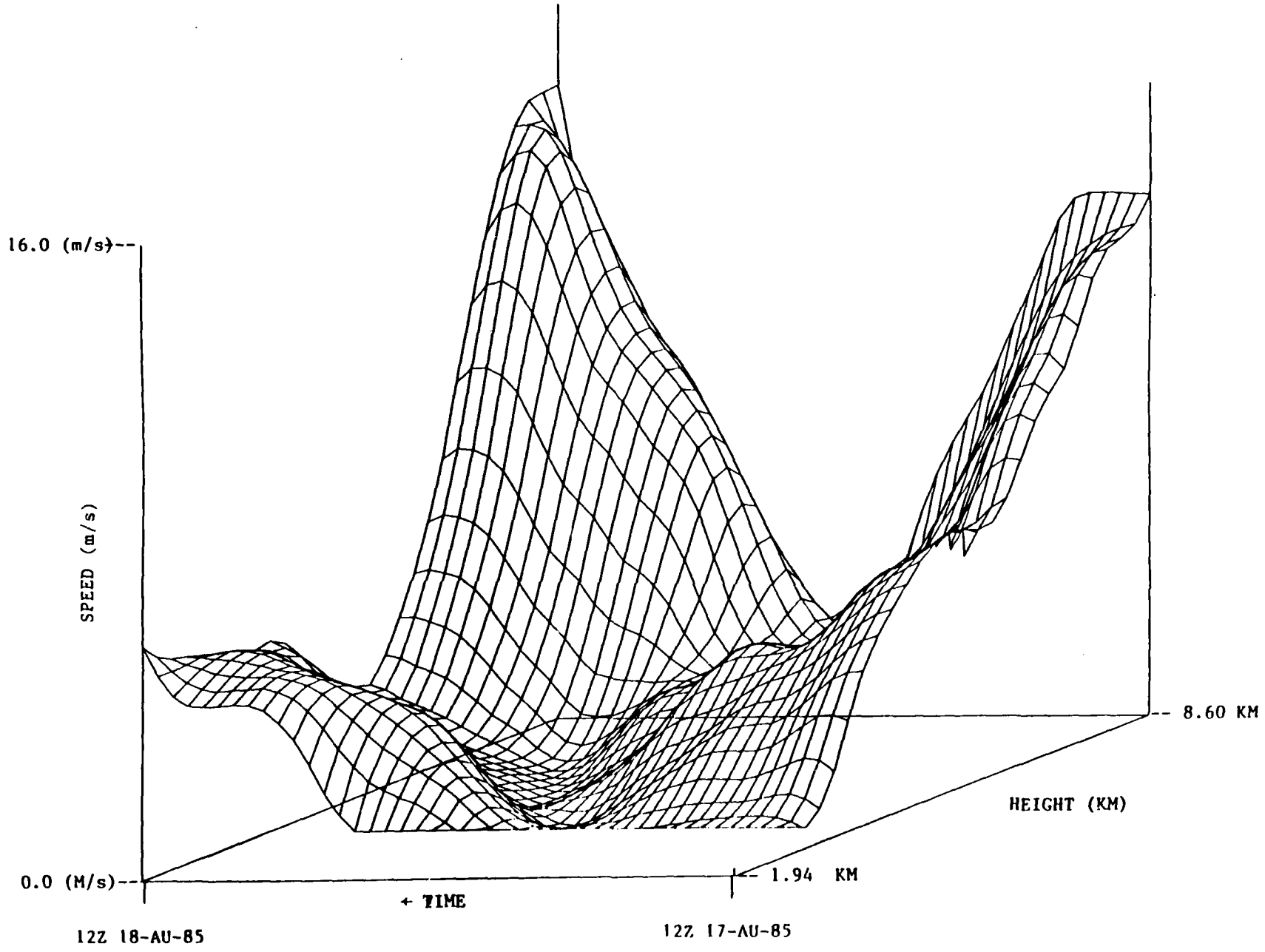

Figure 3 Two dimension plot of wind speed versus time and altitude for the same period as Fig. 2.

APPENDIX B

NOTES CONCERNING THE USE OF CLEAR AIR DOPPLER RADARS FOR THE MEASUREMENT OF C_n^2

Robert M. Peters

Department of Meteorology
The Pennsylvania State University
University Park, PA 16802

Recently the Penn State clear air radar network has been increasingly utilized not only for wind profiling, but also for the measurement of the refractive structure coefficient associated with isotropic turbulence, C_n^2. This coefficient is related to received power amplitude of active indirect sensing systems when signal backscatter is caused solely by refractive index variations due to isotropic turbulence. The physical mechanisms associated with this backscatter in the atmosphere are described in detail by WESELY (1976).

The present Penn State clear air radar network consists of two VHF (6M wavelength) Doppler radars and a transportable UHF (75 CM wavelength) Doppler radar. The systems are designed primarily for wind profiling of the troposphere and stratosphere. The Penn State network is described by THOMSON et al. (1984) and is based upon the concepts, signal processing hardware designs and software provided by

the NOAA/ERL Wave Propagation Lab (STRAUCH et al., 1984). An ongoing experimental research effort at Penn State pertains to measurements of turbulent backscatter from radars, optical systems, acoustic systems and direct measurements of turbulence via aircraft and thermosondes. During a recent experiment, one VHF radar was used for this purpose and measurements of the VHF structure coefficient were obtained (MOSS, 1986). It has become evident that the quantitative measurement of radar system power parameters that are required for the determination of C_n^2 are prone to errors that are frequently not addressed in designs that are optimized for Doppler measurements.

In order for backscattered power to be related to isotropic turbulence, it must be known that the received signal amplitude is not modified by other backscatter sources, reflections or interference from other emitters. Continuous interference is usually man made from sources such as arcing power lines, radio transmissions or broadband noise from the digital systems of the radar. Good site selection and radar system engineering practices will prevent interference from these types of emission. Hard targets will cause undesired reflections. Reflections due to ground clutter may be partially eliminated in spectral processing but are best avoided by choosing radar sites that have no large targets visible at distances comparable to the radar's range response. Hard reflections from aircraft will override the atmospheric backscattered signal. The consensus algorithm used for averaging in the Penn State radar software (STRAUCH et al., 1984) will eliminate the short term occurrence of aircraft reflections from an averaged data set. However, the location of major airways should be a factor during radar site selection. Enhanced signal returns from the atmosphere from other natural sources of

anisotropic irregularities will occur with a zenith pointing beam as described by DOVIAK and ZRNIC' (1983). As shown by DOVIAK and ZRNIC' (1983), the response of VHF radars to anisotropic irregularities will be insignificant at a 15 degree off zenith pointing angle, assuming that the layered structure causing the signal enhancement is horizontal. At Penn State, one of the 15 degree off-axis beams of the VHF radar antenna is used for the measurement of C_n^2 as well as for one wind velocity component. Antenna beam side lobe response to enhanced signal returns from the vertical are further reduced by having a zenith null designed into the antenna pattern.

In order to make quantitative measurements of received signal amplitudes, the radar systems's hardware must be calibrated or its calibration inferred from other sources. System hardware for calibration purposes are the antenna system, transmitters, receivers and analog to digital converters used for parameter measurements.

The antenna patterns of large upward pointing VHF phased arrays, such as those used at Penn State, are difficult to measure in their far fields. Computer antenna pattern models are quite accurate with regard to antenna pattern shape. Experience has shown that an antenna will usually have a gain within a few decibels (dB) of that predicted by a validated antenna model, if the antenna is well engineered and installed. Pattern altering metallic objects should not be placed in or near the antenna field if reliance is placed upon previously determined antenna gain figures that are to be used in the measurement of structure parameters. Astronomical noise sources have been used to confirm antenna pointing maxima. Galactic sources are useful in the northern hemisphere (MOSS, 1986) and the sun can be used

in equatorial regions (RIDDLE, 1985). Precise patterns and gains have been determined for the Mu radar facility in Japan by integrating direct satellite measurments as described by SATO et al (1985). The phase and power distribution provided to the elements of the VHF phased array may be directly measured to provide a more accurate input to modeled antenna patterns. The performance of an uncalibrated antenna system may be statistically compared with other systems of known performance and its gain inferred (MOSS, 1986), as long as other system components are calibrated. Computer estimation of C_n^2 may be derived from atmospheric soundings and used to estimate system calibration. A field tested computer model developed by VANZANDT et al. (1981) could possibly be used for this purpose.

Transmitter parameters such as power and pulse width must be known. The Penn State network incorporates transmitters which have internal microprocessor control and monitoring systems. The radar system executive control computer at each site provides a means to remotely monitor and control each radar transmitter in the network. Transmitter power may be monitored via this arrangement, however, this indirect method of measurement is prone to error if the associated electronic circuits are not calibrated. With Penn State systems, the transmitted power level is derived from an adjustable RF voltage monitoring circuit with its output supplied to the analog to digital converter of each transmitter's processor. Each transmitter includes an integral directional coupler. To ensure the accuracy of the transmitter power monitor, the coupling coefficient of each directional coupler should be calibrated and power measurements taken to check and calibrate the microprocessor based power monitoring system.

The receiver system includes not only the radar receivers and preamplifiers, but also the analog to digital converters. For structure parameter measurements, the receiving system gain must be calibrated. For relative power measurements of received signal amplitude, the calibration must be done with test instrumentation. Any changes to the receiving system, such as replacement of a receiver preamplifier, would require recalibration. For radar systems such as the Penn State UHF Doppler radar, this is the most practical method of calibration since the UHF system utilizes one receiver time shared among several antenna pointing angles. The minimun discernable received signal power of the UHF system is limited by the 100 K noise temperature (approximate) of the receiver preamplifier. This type of calibration is unnecessary for the VHF Doppler radars. For these systems, the minimum signal detectabilty is limited by a galactic noise temperature backround in the order of several thousand Kelvins (KO, 1958). For this reason, the galactic noise level is used as an automatic calibration for all receivers at Penn State VHF radar sites. This is accomplished by archiving a spectrally derived estimate of consensus averaged signal to noise ratio (most systems presently archive relative power on a routine basis). Structure parameter errors at close ranges using VHF radar have been observe during recent experiments (MOSS, 1986). The cause for this class of error has not been studied but appears either to be due to a near field antenna response error or receiver dynamic range limiting.

Less than ideal receiver low pass filter stability, calibration and adjustment has been the most significant cause of error of spectrally derived structure parameters from the VHF radars.

Specifically, the presence of DC offsets and gain imbalance between real and quadrature channels will produce a host of errors in spectral signal processing. Each received signal spectrum is actually the result of several averaged spectra, each of which is derived from a time series of coherently integrated received signal amplitudes at each radar altitude. Each signal spectrum is derived from the complex Fast Fourier Transform of the receiver's range gated real and quadrature outputs. Peaks that may occur in each spectrum about the zero frequency line at an equal amplitude at all range gates are usually the result of the presence of a mean or trend in the complex signal data set that is not completely removable by the signal processing software. Image peaks that may occur opposite the spectral peak associated with the clear air signal return usually are a result of dynamic range limiting of the receiving system. A consistent image peak in all range gates is usually associated with a gain or quadrature imbalance between the I and Q channels of the receiving system. Note that the receiving system also includes the analog to digital converters of the signal processing system. Imbalances between the I and Q analog to digital converters will produce the same errors. Errors produced by means, trends and imbalances produce errors in structure parameter data that are not as easily removed as compared to Doppler velocity measurements. The amplitude of a spectral image will always be lower than the true signal so that Doppler peak detecting algorithms will never choose the image peak for Doppler processing. Any means or trends will be have an effect in Doppler velocity processing only if the zero amplitude peak is greater than the clear air peak. If the zero peak is larger, then the artificially constant velocity produced in the beam component (which is frequently blamed on ground clutter) can be easily removed from

wind velocity data sets by computer post processing. The effect of these types of spectral errors in obtaining received signal power or signal to noise ratio are not as obvious. The spectral processing algorithm will include ground clutter peaks as part of the returned backscattered signal at low radial wind velocities. Any image peaks that occur will also bias the estimates of received signal power and possibly produce a velocity bias to the estimate. The presence of spectral images will contribute to the estimated noise level thereby producing errors in the signal to noise ratio.

To reduce the errors associated with the receiver system for all types of measurements, the receivers must be carefully adjusted in the lab for gain balance and zero offsets after a period of stabilization. Software solutions can contribute to the reduction of error. The present software used at Penn State (STRAUCH et al., 1984) removes the mean from the received signal data set. Trend removal is more difficult for the real time nature of our signal processing system however improvements have been suggested by STRAUCH (1986). The ultimate solution is to treat the disease, not the symptoms. The filter and output stages of VHF and UHF Doppler receivers should be designed for maximum amplitude stability as well as frequency stability. The manufacturer of the radio frequency subsystems of the Penn State Doppler radars are now providing improved receivers for new systems and retrofits for present systems to reduce the possibility of these types of problems. The Penn State UHF system will have a programmable attenuator added to the receiver system. This will allow the receiver's gain to be fixed at an ideal level depending upon operating requirements. This feature, along with improved on-line spectral display software, will allow field optimization of radar

parameters to reduce the sources of error described herein. An improved method of spectral signal detection has also been developed (PETERS and WILLIAMS, 1988). The new method provides a better signal peak selection mode in the presence of ground clutter or in low signal to noise conditions. Careful attention to clear air radar system performance will result in better estimates of all measurable clear air parameters.

REFERENCES

Doviak, R. J. and D. S. Zrnic' (1983), Fresnel zone considerations for reflection and scatter from refractive index irregularities, *Handbook for MAP, Vol. 9*, SCOSTEP Secretariat, Dept. of Electrical Engineering, University of Illinois, 83-97.

KO, H. C. (1958), The distribution of cosmic radio backround radiation, *Proc. IRE, Vol. 46*, 208-215.

Moss, M. (1986), Thesis Prospectus, Dept. of Meteorology, Florida State University.

Peters, R. M. and S. Williams (1988), An improved method of clear air signal detection for Doppler wind profiling radars, (in process), Dept. of Meteorology, Penn State University.

Riddle, A. C. (1985), Use of the sun to determine pointing of ST radar beams, *Handbook for MAP, Vol. 20*, SCOSTEP Secretatiat, Dept. of

Electrical Engineering, University of Illinois, 410-413.

Sato, T., Y. Inooka, S. Fukao, and S. Kato (1985), Monitoring of the MU radar antenna pattern by satellite OHZORA (EXOS-C), *Handbook for MAP, Vol. 20,* SCOSTEP Secretariat, Dept. of Electrical Engineering, University of Illinois, 414-418.

Strauch, R. G., D. A. Merritt, K. P. Moran, K. B. Earnshaw, and D. Van de Kamp (1984), The Colorado wind-profiling network, *Journal of Atmospheric and Oceanic Technology, Vol.1,* 37-49.

Strauch, R. G. (1986), Changes to data processing, (Memoranda to users of WPL designed systems, March 27, 1986), Wave Propagation Lab. NOAA/ERL, Boulder, CO.

Thomson, D. W., C. W. Fairall, and R. M. Peters (1984), Network ST radar and related measurements at Penn State University: a progress report, *Handbook for MAP, Vol. 14,* SCOSTEP Secretariat, Dept. of Electrical Engineering, University of Illinois, 350-355.

VanZandt, T. E., K. S. Gage, and J. M. Warnock (1981), An improved model for the calculation of profiles of C_n^2 in the free atmosphere, *20th Conf. on Radar Meteorology,* Boston, MA, 129-135.

Wesely, M. (1976), The combined effect of temperature and humidity fluctuations on refractive index, *Journal of Applied Meteorology, Vol. 15,* 43-49.